Quantum evolution of black hole initial data sets: Foundations

Emanuele Alesci,[1,*] Sina Bahrami,[1,†] and Daniele Pranzetti[2,‡]
[1]Institute for Gravitation and the Cosmos, Pennsylvania State University, University Park, Pennsylvania 16802, USA
[2]Perimeter Institute for Theoretical Physics, Waterloo, Ontario N2L 2Y5, Canada

(Received 26 July 2018; published 15 August 2018)

We construct a formalism for evolving spherically symmetric black hole initial data sets within a canonical approach to quantum gravity. This problem can be formulated precisely in quantum reduced loop gravity, a framework which has been successfully applied to give a full theory derivation of loop quantum cosmology. We extend this setting by implementing a particular choice of partial gauge which is then used to select a kinematical Hilbert space where the symmetry reduction is imposed through semiclassical states. The main result of this investigation is an effective Hamiltonian that can be used to solve for quantum black hole geometries by evolving classical black hole initial data sets.

DOI: 10.1103/PhysRevD.98.046014

I. INTRODUCTION

Singularities are generic predictions of general relativity; this was the conclusion of the first singularity theorem that was discovered by Roger Penrose in 1964 [1]. Prior to this, it was widely suspected that singularities are aspects of algebraically special spacetimes or end results of highly symmetric processes [2], as in the gravitational collapse of a spherically symmetric compact object [3]. Penrose's arguments instead attributed the occurrence of singularities to the formation of trapped surfaces in geometries where the Ricci curvature tensor satisfies $R_{ab}k^a k^b \geq 0$ for all null vectors $\vec{k}$.[1] Further progress concerning the formation of singularities in general relativity was subsequently made by the landmark theorems of Hawking and Penrose [4,5].[2]

Despite their robustness, singularity theorems are reliable only in the regime where spacetime geometry is classical. This, however, runs contrary to what they set out to accomplish. In fact, one expects quantum corrections to classical geometry to become relevant on scales where $|R_{abcd}R^{abcd}| \gtrsim l_p^{-4}$, where R_{abcd} is the Riemann curvature tensor and $l_p \sim 10^{-33}$ cm is the Planck length. For the most elementary examples of singularity in general relativity, $|R_{abcd}R^{abcd}|$ blows up as one approaches the singularity. Therefore, whether singularities generically form in nature as predicted by the singularity theorems hinges on how spacetime behaves in the quantum domain.

The degree to which quantum effects modify classical singularities has long been a subject of speculation. Penrose argued in [7] that understanding the quantum structure of the initial spacetime singularity is the key to resolving one of the long-standing puzzles in theoretical physics, namely the second law of thermodynamics and the origin of the observed (albeit minute) time asymmetry in nature.[3] Should quantum effects resolve this initial spacetime singularity by replacing it with a bounce, it may be difficult to concoct a compelling explanation for the second law of thermodynamics [11].[4,5] However, in the context of quantum geometry, one expects the notion of entropy and how it evolves to be scale dependent. Therefore, the fate of the second law in quantum gravity is tied to understanding the quantum structure of the Universe near the cosmological singularities as well as the exact mechanism by which the classical and continuous spacetime manifold emerges from them.

Aside from cosmological singularities, one can also ponder upon consequences of black hole singularities being removed by quantum effects. In that case, a resolution for a number of outstanding riddles and open questions may be within reach. Of significant importance are the cosmic censorship hypothesis [14] and the information loss paradox of black hole evaporation [15]. For the latter, if the

*eza69@psu.edu
†sina.bahrami@psu.edu
‡dpranzetti@perimeterinstitute.ca

[1]Penrose's theorem requires global hyperbolicity for the spacetime.

[2]See [6] for an extensive discussion of these results.

[3]A microscopic example of this time asymmetry is the CP-violating decay of K^0 mesons [8–10].

[4]We refer the interested reader to [7] where the vanishing Weyl curvature hypothesis is explained.

[5]Steinhardt and Turok have argued in [12,13] that in ekpyrotic models the second law of thermodynamics is respected; the total entropy increases from cycle to cycle while the entropy density undergoes periodic behavior. Nonetheless, ekpyrotic models do not provide any explanations for the origin of the second law.

semiclassical approximation scheme is correct, the unitarity principle of quantum mechanics is violated by pure states evolving into mixed states during black hole evaporation (see [16] for a review of the basic arguments). Several ideas have been proposed to resolve this paradox with some being more radical than others. On the more exotic side, there are ideas proposing black hole event horizons turning into "firewalls" [17] or "fuzzballs" [18]. In these speculative scenarios, phenomena in gross violation of the equivalence principle are required to occur on a black hole event horizon in order to shut down correlations between the infalling and outgoing pair of created particles. On the more conservative end of the spectrum, there are proposals such as Planck-sized remnants of the evaporation process [19,20], and singularity resolution by quantum gravity effects that lead to an extension of the spacetime diagram for evaporating black holes [21]. However, a clear-cut resolution to the aforementioned paradox has not yet emerged in these latter proposals either. Indeed the idea of black hole remnants has been criticized for a lack of viability as it requires a Planck-sized object to have an enormous entropy, roughly on the order of M^2 where M is the black hole mass, which in turn leads to the infinite pair production problem, although objections have been raised against this critique in the literature (see, e.g., [16,22–24] for a discussion). Similarly in the case where the black hole singularity is resolved and a classical spacetime emerges to the causal future of the would-be singularity, a description for a concrete mechanism that purifies the early radiation degrees of freedom (d.o.f.) is lacking (see, however, [25] for an interesting proposal). Beyond all speculations, a definitive fate of a classical singularity is only predicted by a detailed full quantum gravity calculation. Given the intimate relation between the last stages of black hole evaporation and Planck-scale physics, this paradox will likely be resolved by a better understanding of a quantum gravity description.

Presently, string theory and loop quantum gravity (LQG) have been sufficiently developed to allow for problems of this kind to be explored within their respective frameworks. In the past two decades some evidence has emerged in string theory in favor of quantum singularity resolution. One of the earliest results is by Horowitz *et al.* [26] where AdS/CFT duality was used to argue that the interior of a black hole in anti–de Sitter space is described by a singularity-free supersymmetric field theory on the boundary. Similar results have been obtained for cosmological singularities using the AdS/CFT duality [27–30]. Aside from AdS/CFT, other well-known proposals include models with tachyon condensation [31,32], matrix models [33,34], and models that use orientifolds [35]. Nevertheless, no full theory calculation has been produced that can provide a definitive answer.

LQG [36] embodies the most studied nonperturbative quantization program of the gravitational field. Questions such as the quantum fate of classical spacetime singularities can in principle be formulated and investigated within this framework [37,38]. On the specific subject of black hole singularities, a number of very important studies [39–47] have been conducted where the primary focus is on the geometry interior to the event horizon of a Schwarzschild black hole. The aforementioned geometry is homogeneous and can be described by the Kantowski-Sachs type metric. This particular geometry can be treated as a minisuperspace for which the techniques developed in the cosmological context by loop quantum cosmology (LQC) [48–50] are available and can be readily used. The results of these investigations point to a singularity resolution of the bouncing cosmological type [51–53]. Further evidence of singularity resolution due to the implementation of the LQG dynamics was provided also in [54,55].

The study of the complete phase space in the symmetry reduced case started with the work of Kuchar [56] in metric variables and the work of Thiemann and Kastrup [57] in complex Ashtekar variables which was then revised using LQG techniques [58]. In [59–61] the Ashtekar-Barbero connection was used to obtain a kinematical description along with the Hamiltonian constraint. In [62,63] the extension of the previous results within a classical modification of the Dirac algebra that transforms the symmetry reduced case in a Lie algebra allowed one to define the physical Hilbert space and observables corresponding to a metric that was shown to be free of singularity.

A parallel line of investigation was conducted within the framework of covariant LQG, namely the spinfoam models [64]. The idea is that if the singularity is removed as in the homogeneous LQC, it is reasonable to expect a black hole–white hole transition named a Planck star [65] that can be modeled with a nonsingular metric [66,67] of the Hayward type [68]. The tunneling can then be studied in terms of transition amplitudes between coherent states representing classical spacetimes [69,70]. Phenomenological consequences were discussed in [71–73].

An alternative approach to model semiclassical and continuous spherically symmetric geometry has recently been pursued within the framework of group field theory (GFT) [74] in its operatorial formulation, providing a second quantized version of LQG. The main idea behind this approach is to describe homogeneous continuum geometries in terms of GFT condensate states encoding the information in a condensate wave function depending on a few collective variables [75]. This allows one to model a black hole geometry by starting from the full theory and implementing the symmetry reduction at the quantum level [76,77]. In this case, application of the GFT condensates formalism to the cosmological setting has allowed one to recover modified Friedmann equations showing the presence of a bounce in the Planck regime [78–82]. One could then hope that also for the black hole case singularity resolution could be proven. However, implementation of

the GFT dynamics in the black hole context is currently out of reach due to the highly challenging technical difficulties when dealing with generalized condensate states implementing graph connectivity. The main achievement of this manuscript is to show how to successfully implement the LQG dynamics to the case of a spherically symmetric black hole geometry while starting from the full theory and keeping the graph structure.

In this article we adopt the so-called quantum reduced loop gravity (QRLG) [83–91] approach and apply it to spherically symmetric geometries. At the heart of this approach lies the old familiar idea that a choice of symmetry compatible coordinate system drastically simplifies the task of solving the Einstein equations. QRLG intends to carry this simplification to the quantum level. To understand this better, it is helpful to briefly review how this framework has been applied to homogeneous anisotropic cosmologies.

In the case of Bianchi I spacetime, the existence of three Killing vector fields allows one to choose a coordinate system in which the metric is diagonal and only dependent on the time variable. The space of Bianchi I metrics is then just a subspace of the full Arnowitt-Deser-Misner (ADM) phase space that consists of homogeneous and diagonal 3-metrics. Note that diagonalizing 3-metrics is always achievable by imposing a partial gauge fixing (i.e., by using the gauge freedom provided by the spatial diffeomorphisms [92,93]), which comes at the cost of dealing with second class constraints and selecting a partially reduced phase space. A subspace of the latter is coordinate independent metrics singled out by symmetry. The classical use of a minisuperspace can thus be seen as first reaching the partially reduced phase space and then restricting it to its symmetric sector. The QRLG approach to cosmology was devoted to access this sector at the quantum level as opposed to LQC, in which the symmetry reduction is performed classically and one is then left with finite-dimensional systems. The main reason for this extra step is that the fundamental structure of LQG does not permit one to use differential geometry to define the notion of symmetry at the quantum level. In the process of symmetry reduction followed by quantization (as required in LQC) most of the structure of the full Hilbert space is lost and has to be reintroduced via assumptions.

The QRLG approach is to revert the process of symmetry reduction and quantization to derive a symmetric sector of LQG in which none of the fundamental structures of the full theory is lost. To achieve this goal, a reduced Hilbert space is first selected from the full kinematical Hilbert space for which the metric is diagonal and then the symmetry reduction is performed, selecting homogeneous coherent states. This procedure allows one to work with the complete structure of the full theory, consisting of quantum states of polymeric nature labeled by graphs and $SU(2)$ representations. Moreover, it shows that the minisuperspace effective quantization of LQC can be reproduced at the level of the expectation values of quantum operators acting on the partially gauge fixed Hilbert space. However, the presence of the graphs also leads to some modification in the deep Planckian regime.

Here we intend to apply the same construction to spherically symmetric geometries. We will do this in four steps: in the first step, we implement the gauge fixing condition at the quantum level to define the partially gauge fixed Hilbert space.[6] This corresponds to the classical reduced phase space for a suitable choice of gauge that results in the triad E^a_i having only the five components E^r_3, E^θ_1, E^θ_2, E^ϕ_1, E^ϕ_2. In terms of the 3-metric, this partial gauge choice amounts to having only the rr, $\theta\theta$, $\theta\phi$ and $\phi\phi$ components as nonzero. In the second step, we project the constraints defined in the full theory to represent the classical gauge unfixed constraints [97]. The third step is to define states belonging to this kinematical Hilbert space where the classical notion of symmetry can be defined using spherically symmetric coherent states. Finally, we define the effective constraints by taking the expectation value of the quantum reduced constraints on the symmetry reduced states.

This article is organized as follows. In Sec. II we review the canonical formulation of general relativity when restricted to spherically symmetric geometries. In Sec. III we show how this symmetric phase space can be seen as a subspace of a partially gauge fixed phase space. We work out the first class constraint algebra obtained from the gauge unfixing procedure that preserves this subspace. In Sec. IV we build the reduced kinematical Hilbert space that implements at the quantum level this partial gauge fixing. We then derive the Hamiltonian constraint operator acting on this Hilbert space in Sec. V. After this, we build the semiclassical states representing spherically symmetric states in Sec. VI. Finally in Sec. VII we derive the effective Hamiltonian by taking the expectation value of the reduced Hamiltonian constraint evaluated on the coherent states. Further technical details are presented in Appendices A and B; Appendix C contains an alternative approach to the quantization of the Lorentzian part of the Hamiltonian constraint.

II. CANONICAL FORMULATION IN ASHTEKAR VARIABLES FOR GEOMETRIES IN SPHERICAL SYMMETRY

The ADM formalism [98] describes the Hamiltonian evolution of initial data sets in general relativity. In this

[6]Recent studies [94–96] attempted to provide a quantization for the reduced phase space in a radial gauge for the ADM variables different from the one introduced in [97] for connection variables. In [96] a scheme to implement symmetry reduction at the quantum level was also introduced; however, this analysis relies on a Peldan hybrid connection, yielding a description of the kinematical Hilbert space in terms of point holonomies and a restricted action of the Hamiltonian constraint to a single point for a given 2-sphere.

context, a vacuum initial data set consists of a spacelike Cauchy surface[7] Σ_t together with its intrinsic metric q_{ab} and a symmetric tensor π^{ab} that are required to satisfy

$$\frac{{}^{(3)}R}{\kappa^2} - q^{-1}\pi^{ab}\pi_{ab} + \frac{1}{2}q^{-1}\pi^2 = 0,$$
$$D_a(q^{-1/2}\pi^{ab}) = 0, \tag{1}$$

on Σ_t. Here D_a is the q_{ab} compatible torsion-free derivative operator, $\kappa \equiv 8\pi G$, $q \equiv \det(q_{ab})$, and $\pi \equiv q_{ab}\pi^{ab}$. Once embedded in a four-dimensional spacetime, π^{ab} is related to the extrinsic curvature K_{ab} of Σ_t by

$$\pi^{ab} = \frac{1}{\kappa}\sqrt{q}(K^{ab} - Kq^{ab}). \tag{2}$$

The canonical phase space variables, namely q_{ab} and π^{ab}, are evolved by the relevant Hamiltonian (to be described below) and are subject to the following Poisson bracket:

$$\{\pi^{ab}(t,\mathbf{x}), q_{cd}(t,\mathbf{y})\} = \kappa\delta^a_{(c}\delta^b_{d)}\delta^3(\mathbf{x}-\mathbf{y}) \tag{3}$$

at all times. Note that not all components of q_{ab} and π^{ab} are independent; of 12 components, 4 can be eliminated by a choice of coordinate gauge and another 4 are eliminated by virtue of Eq. (1). This leaves two propagating d.o.f. for the gravitational field as expected.

The intrinsic metrics on all Σ_t can be sewed together to provide a spacetime metric given by

$$ds^2 = -N^2dt^2 + q_{ab}(dx^a + N^a dt)(dx^b + N^b dt), \tag{4}$$

where N is the lapse function and N^a is the shift vector. A choice of N and N^a determines a foliation for the spacetime. One needs to specify a foliation prior to solving the Hamilton's equations for q_{ab} and π^{ab}.

Here we are interested in the case where Σ_t has the topology $\Sigma_t = \mathbb{R}\times S^2$ and the spacetime geometry is assumed to be spherically symmetric. The most generic spacetime metric is then given by

$$ds^2 = -N^2dt^2 + \Lambda^2(dr + N^r dt)^2 + R^2(d\theta^2 + \sin^2\theta d\varphi^2), \tag{5}$$

where N, N^r, R, Λ are functions of r and t, with $-\infty < t$, $r < \infty$. $\Lambda(t,r)$ and $R(t,r)$ are assumed to be positive functions; together with their conjugate momenta they represent the set of phase space canonical variables. Note that it follows from the above equation that the intrinsic metric on the spacelike hypersurfaces is

$$d\sigma^2 = \Lambda^2 dt^2 + R^2(d\theta^2 + \sin^2\theta d\varphi^2). \tag{6}$$

Expectedly, once a foliation is chosen, two independent functions are sufficient to describe an arbitrary metric in spherical symmetry.

As it turns out, the canonical quantization program is most conveniently formulated in terms of the Ashtekar-Barbero connection A^i_a and the densitized triad E^a_i instead of q_{ab} and π^{ab}.[8] This way, deriving the quantum corrected semiclassical Hamiltonian is significantly more straightforward, as will be shown in the subsequent sections. The spatial index a runs over $\{r,\theta,\varphi\}$, while the $SU(2)$ internal index $i \in \{1,2,3\}$. One then has the following Poisson bracket:

$$\{A^i_a(\mathbf{x}), E^b_j(\mathbf{y})\} = \kappa\gamma\delta^i_j\delta^b_a\delta^3(\mathbf{x}-\mathbf{y}) \tag{7}$$

in lieu of Eq. (3). Note that here $\delta^3(\mathbf{x}-\mathbf{y}) \equiv \delta(r_{\mathbf{x}} - r_{\mathbf{y}})\delta(\theta_{\mathbf{x}} - \theta_{\mathbf{y}})\delta(\varphi_{\mathbf{x}} - \varphi_{\mathbf{y}})$ and γ is the Barbero-Immirzi parameter.

To derive the densitized triad, we begin by deriving the tetrad e^I_α for the metric (5). This is done using the relation $g_{\alpha\beta} = e^I_\alpha e_{I\beta}$. A quick calculation reveals

$$g_{tt} = -N^2 + \Lambda^2(N^r)^2 = -(e^0_t)^2 + (e^3_t)^2,$$
$$g_{tr} = \Lambda^2 N^r = -e^0_t e^0_r + e^3_t e^3_r,$$
$$g_{rr} = \Lambda^2 = -(e^0_r)^2 + (e^3_r)^2,$$
$$g_{\theta\theta} = R^2 = e^1_\theta e_{1\theta} + e^2_\theta e_{2\theta},$$
$$g_{\varphi\varphi} = R^2(\sin\theta)^2 = e^1_\varphi e_{1\varphi} + e^2_\varphi e_{2\varphi},$$
$$g_{\theta\varphi} = 0 = e^1_\theta e_{1\varphi} + e^2_\theta e_{2\varphi},$$

from which we read off the complete set of tetrad components

$$e^0 = Ndt, \tag{8a}$$

$$e^3 = \Lambda N^r dt + \Lambda dr, \tag{8b}$$

$$e^1 = R\cos\tilde{\alpha}d\theta - R\sin\theta\sin\tilde{\alpha}d\varphi, \tag{8c}$$

$$e^2 = R\sin\tilde{\alpha}d\theta + R\sin\theta\cos\tilde{\alpha}d\varphi. \tag{8d}$$

Here we have left a rotation freedom for the components e^1 and e^2 described by the angle $\tilde{\alpha}$, which can have any arbitrary given value. The tetrad components also satisfy the following equations:

[7] Σ_t represents an instant of time in the spacetime M. One tacitly assumes that $M = \mathbb{R}\times\Sigma_t$.

[8] See [99] for a thorough exposition on the subject.

$$e^0_r e^r_3 + e^0_t e^t_3 = 0,$$
$$e^1_\theta e^\theta_2 + e^1_\varphi e^\varphi_2 = 0.$$

If we go to the time gauge where $e^0_a = n_a$, the densitized triad

$$E = E^a_i \tau^i \partial_a, \quad \text{where } E^a_i = \frac{1}{2}\epsilon^{abc}\epsilon_{ijk} e^j_b e^k_c, \tag{9}$$

becomes

$$E = R^2 \sin\theta \tau^3 \partial_r + \Lambda R \sin\theta(\cos\tilde{\alpha}\tau^1 + \sin\tilde{\alpha}\tau^2)\partial_\theta + \Lambda R(\cos\tilde{\alpha}\tau^2 - \sin\tilde{\alpha}\tau^1)\partial_\varphi. \tag{10}$$

Here τ^i are basis vectors in the internal space.[9]

The connection components $\omega^{IJ}_a = -\omega^{JI}_a$ can be computed from the torsion-free condition $de^I = -\omega^I{}_J \wedge e^J$. The explicit derivation is provided in Appendix A. Using the result of Eqs. (A3a), the Ashtekar-Barbero connection $A^i = \Gamma^i + \gamma K^i$, where $\Gamma^i = -\frac{1}{2}\epsilon^i{}_{jk}\omega^{jk}$ and $K^i = \omega^{0i}$, is given by

$$\begin{aligned} A &= A^i_a \tau_i dx^a \\ &= -\gamma\frac{(\Lambda' N^r + \Lambda N^{rt} - \dot{\Lambda})}{N}\tau_3 dr + \frac{R'}{\Lambda}\left\{\left[\gamma\left(N^r - \frac{\dot{R}}{R'}\right)\sin\tilde{\alpha} + \cos\tilde{\alpha}\right]\tau_2 + \left[\gamma\left(N^r - \frac{\dot{R}}{R'}\right)\cos\tilde{\alpha} - \sin\tilde{\alpha}\right]\tau_1\right\} d\theta \\ &\quad + \frac{\sin\theta R'}{\Lambda}\left\{\left[\gamma\left(N^r - \frac{\dot{R}}{R'}\right)\cos\tilde{\alpha} - \sin\tilde{\alpha}\right]\tau_2 - \left[\gamma\left(N^r - \frac{\dot{R}}{R'}\right)\sin\tilde{\alpha} + \cos\tilde{\alpha}\right]\tau_1\right\} d\varphi + \cos\theta\tau_3 d\varphi. \end{aligned} \tag{11}$$

If one is to use the notation of [61], where the spherically symmetric Ashtekar-Barbero connection and triad are written as

$$E = E^r(t,r)\sin\theta\tau_3\partial_r + [E^1(t,r)\tau_1 + E^2(t,r)\tau_2]\sin\theta\partial_\theta + [E^1(t,r)\tau_2 - E^2(t,r)\tau_1]\partial_\varphi, \tag{12}$$

$$A = A_r(t,r)\tau_3 dr + [A_1(t,r)\tau_1 + A_2(t,r)\tau_2]d\theta + \sin\theta[A_1(t,r)\tau_2 - A_2(t,r)\tau_1]d\varphi + \cos\theta\tau_3 d\varphi, \tag{13}$$

one has

$$E^r(t,r) = R^2, \quad E^1(t,r) = \Lambda R\cos\tilde{\alpha}, \quad E^2(t,r) = \Lambda R\sin\tilde{\alpha}, \tag{14}$$

$$A_r(t,r) = -\gamma\frac{(\Lambda' N^r + \Lambda N^{rt} - \dot{\Lambda})}{N}, \tag{15}$$

$$A_1(t,r) = \frac{R'}{\Lambda}\left[\gamma\left(N^r - \frac{\dot{R}}{R'}\right)\cos\tilde{\alpha} - \sin\tilde{\alpha}\right], \tag{16}$$

$$A_2(t,r) = \frac{R'}{\Lambda}\left[\gamma\left(N^r - \frac{\dot{R}}{R'}\right)\sin\tilde{\alpha} + \cos\tilde{\alpha}\right]. \tag{17}$$

The Poisson bracket (7) then takes the form

$$\{A_r(t,r), E^r(t,r')\} = 2G\gamma\delta(r-r'), \tag{18a}$$

$$\{A_1(t,r), E^1(t,r')\} = G\gamma\delta(r-r'), \tag{18b}$$

$$\{A_2(t,r), E^2(t,r')\} = G\gamma\delta(r-r'). \tag{18c}$$

III. CONSTRAINTS FOR THE PARTIALLY GAUGE FIXED PHASE SPACE

In this section we derive the classical Hamiltonian, diffeomorphism, and gauge constraints subject to the particular gauge fixing scheme of [97].

The classical phase space is characterized by the following standard seven constraints

$$\kappa G_i = \partial_a E^a_i + \epsilon_{ij}{}^k A^j_a E^a_k, \qquad \text{Gauss constraint} \tag{19a}$$

$$\kappa H_a = F^i_{ab} E^b_i - A^i_a G_i, \qquad \text{Diffeomorphism constraint} \tag{19b}$$

$$\kappa H = \frac{E^a_i E^b_j}{\sqrt{\det(E)}}\left[\epsilon^{ij}{}_k F^k_{ab} - 2(1+\gamma^2)K^i_{[a}K^j_{b]}\right], \qquad \text{Hamiltonian constraint} \tag{19c}$$

where

$$F^i_{ab} = \partial_a A^i_b - \partial_b A^i_a + \epsilon^i{}_{jk} A^j_a A^k_b \tag{20}$$

are the curvature components of the Ashtekar-Barbero connection. Notice that when we substitute the triad and

[9] We use the anti-Hermitian basis τ_i, where $[\tau_i, \tau_j] = \epsilon_{ij}{}^k\tau_k$ and $(\tau_i)^2 = -\frac{1}{4}\mathbb{I}$ for all i's and $\mathrm{Tr}(\tau_i\tau_j) = -\frac{1}{2}\delta_{ij}$.

the connection given in Eqs. (10) and (11) in the above constraints, we are merely left with the Gauss constraint in the $3 = r$ direction, the radial diffeomorphism constraint, and the Hamiltonian constraint.

In [97] we performed the Dirac treatment of this constrained system when the following radial partial gauge fixing conditions are introduced:

$$E^r_I = 0, \qquad I = 1, 2, \tag{21a}$$

$$E^A_3 = 0, \qquad A = \theta, \phi. \tag{21b}$$

These conditions can be seen as additional constraints in the phase space which render the Hamiltonian system to be of second class. Instead of building the Dirac bracket to impose the second class constraints, in [97] we followed an alternative strategy that goes under the name of a "gauge unfixing" procedure (GU) [100–102]. This procedure, which also requires the inversion of the Dirac matrix, allows us to use the Poisson bracket given in Eq. (7) for imposing the remaining three first class constraints. However, while one of these constraints still corresponds to the original $i = 3$ component of the Gauss constraint, the other two are given by the reduced phase space part of the radial diffeomorphism constraint given in Eq. (19) and the Hamiltonian constraint in Eq. (19c) plus extra terms. Explicitly, denoting with a tilde the extended[10] representation of these remaining constraints, we have

$$\tilde{G}_3[\alpha_3] = {}^R G_3[\alpha_3] = \frac{1}{\kappa}\int d^3x \alpha_3 [\partial_r E^r_3 + \epsilon_{3I}{}^J A^I_B E^B_J], \tag{22}$$

$$\tilde{H}_r[N^r] = \frac{1}{\kappa}{}^R H_r[N^r] + \frac{1}{\kappa}\int d^3x (\partial_A N^r)\left[\frac{\epsilon^{IJ} E^A_I \partial_B E^B_J}{E^r_3} + \frac{\delta^{IJ} E^A_I E^B_J \mathcal{I}_B}{(E^r_3)^2}\right], \tag{23}$$

$$\tilde{H}_E[N] = \frac{1}{\kappa}\int d^3x \frac{N}{\sqrt{\det(E)}}\left[{}^R H_3 - \gamma\left\{\frac{\mathcal{I}_A E^A_I \mathcal{I}_B E^{IB}}{(E^r_3)^2} + \epsilon^{IJ}\frac{E^A_I(\partial_B E^B_J)\mathcal{I}_A}{E^r_3} + \epsilon^{IJ} E^A_I \mathcal{I}_B \partial_A\left(\frac{E^B_J}{E^r_3}\right) - E^r_3 E^A_I \partial_A\left(\frac{\partial_B E^{IB}}{E^r_3}\right)\right\}\right], \tag{24}$$

$$\tilde{H}_L[N] = -2\frac{(1+\gamma^2)}{\kappa}\int d^3x \frac{N {}^R H_L}{\sqrt{\det(E)}}, \tag{25}$$

where α_3 is the $i = 3$ component of the α_i smearing function associated with the Gauss constraint, ${}^R H_r$ is the reduced radial diffeomorphism

$${}^R H_r = (\partial_r A^I_A) E^A_I - A^3_r \partial_r E^r_3, \tag{26}$$

${}^R H_E$ is the reduced Euclidean Hamiltonian

$${}^R H_E = E^r_3 E^A_I \epsilon^I{}_J \partial_r A^J_A + E^A_I E^B_J A^I_{[A} A^J_{B]} + E^r_3 E^A_I A^3_r A^I_A, \tag{27}$$

and ${}^R H_L$ is the reduced Lorentzian Hamiltonian

$${}^R H_L = E^A_I E^B_J K^I_{[A} K^J_{B]} + E^r_3 E^A_I K^3_r K^I_A. \tag{28}$$

To shorten the notation, in the expressions above we have defined

$$D_A \equiv E^B_I \partial_A A^I_B - \partial_B (A^I_A E^B_I), \tag{29}$$

$$\mathcal{I}_A \equiv \int_0^r dr' [D_A + E^r_3 \partial_A A^3_r]_{r'}. \tag{30}$$

Notice that the Lorentzian part of the Hamiltonian constraint does not pick up any extra contribution in addition to the reduced term. This is because, once projected on the gauge surface described by Eq. (21), the Lorentzian term given in Eq. (19) does not contain any extrinsic curvature component conjugate to the flux (i.e., triad) components that we have gauge fixed; therefore, in the gauge unfixing procedure of [97], we do not have to perform any substitution of extended momenta inside H_L.

The Hamiltonian constraint that appears in Eq. (19) can also be written as

$$\kappa H = \frac{s}{\gamma^2}\left[\frac{\epsilon^{ij}{}_k E^a_i E^b_j F^k_{ab}}{\sqrt{\det(E)}} + \left(1 - \frac{\gamma^2}{s}\right)\sqrt{\det(E)} R\right], \tag{31}$$

where $s = \pm$ is the spacetime metric signature, R is the Ricci scalar given by

$$R = R_{ab}{}^{ij} e^a_i e^b_j = -\epsilon_{ijk} R^k_{ab} e^a_i e^b_j, \tag{32}$$

[10]The connotation "extended" refers to the fact that the new expressions for the constraints are obtained by replacing the connection components conjugate to the triad components that we have gauge fixed with their extended versions. This results from solving the second class constraints explicitly. In fact, in [97] it was shown that this corresponds to adding a linear combination of second class constraints to the original H_r and H so that the new expressions preserve the gauge conditions. Effectively, this gauge unfixing procedure amounts to having a new set of first class constraints, equivalent to the initial one, but now written as functionals of only the reduced phase space coordinates.

with

$$R^k_{ab} = 2\partial_{[a}\Gamma^k_{b]} + \epsilon^k{}_{lm}\Gamma^l_a\Gamma^m_b. \tag{33}$$

As we will see in Sec. IV, our aim is to build the QRLG quantum theory where we will access the reduced phase space using projectors from the full theory. Therefore we are not going to perform the reduced phase space quantization as attempted in the existing literature. This means that if we had the physical Hilbert space of the full theory, namely the kernel of the quantum operators corresponding to the constraints given in Eq. (19), we would simply transform it to the Hilbert space of QRLG. Unfortunately, while the structure of the solutions to the Gauss and the vector constraints are very well understood in the full theory [36,103,104], very little is known about the structure of the Hamiltonian constraint [105,106] and its kernel [107,108]. Our strategy is then to use the projector on the kernel of the Gauss and the vector constraints and instead quantize the reduced Hamiltonian constraint. In particular our final aim in this paper is not to find the full set of solutions but just to derive the effective reduced Hamiltonian constraint when the symmetry reduction is imposed at the level of coherent states. To this end, we will compute in the next section the reduced Hamiltonian constraint for spherically symmetric geometry.

A. Symmetric subspace of the reduced phase space: Hamiltonian

Using the curvature components of the Ashtekar-Barbero connection that we worked out in Eq. (A7), the spherically symmetric Euclidean part of the Hamiltonian constraint reduces to

$$\begin{aligned}
H^E_{\rm sph}[N] &= \frac{1}{\kappa}\int_\Sigma d^3x N(x)\frac{E^a_i E^b_j}{\sqrt{\det(E)}}\epsilon^{ij}{}_k F^k_{ab}(A)\\
&= \frac{1}{\kappa}\int_\Sigma d^3x \frac{N(x)}{\sqrt{(E^\theta_1 E^\varphi_2 - E^\theta_2 E^\varphi_1)E^r_3}}[E^r_3(E^\theta_1 F^2_{r\theta}(A) - E^\theta_2 F^1_{r\theta}(A) + E^\varphi_1 F^2_{r\varphi}(A) - E^\varphi_2 F^1_{r\varphi}(A)) + (E^\theta_1 E^\varphi_2 - E^\theta_2 E^\varphi_1)F^3_{\theta\varphi}(A)]\\
&= \frac{1}{\kappa}\int_\Sigma d^3x \frac{N(x)\sin\theta}{\sqrt{((E^1)^2+(E^2)^2)E^r}}[2E^r A_r(E^1 A_1 + E^2 A_2) + 2E^r(E^1 A'_2 - E^2 A'_1) + ((E^1)^2+(E^2)^2)((A^2_1+A^2_2)-1)].
\end{aligned} \tag{34}$$

On the other hand, the reduced Euclidean Hamiltonian given in Eq. (27) yields

$$\begin{aligned}
{}^R H^E[N] &= \frac{1}{\kappa}\int_\Sigma d^3x \frac{N}{\sqrt{\det(E)}}[E^r_3 E^A_I A^3_r A^I_A + E^r_3 E^A_I \epsilon^I{}_J \partial_r A^J_A + E^A_I E^B_J A^I_{[A} A^J_{B]}]\\
&= \frac{1}{\kappa}\int_\Sigma d^3x \frac{N(x)\sin\theta}{\sqrt{((E^1)^2+(E^2)^2)E^r}}[2E^r A_r(E^1 A_1 + E^2 A_2) + 2E^r(E^1 A'_2 - E^2 A'_1) + ((E^1)^2+(E^2)^2)(A^2_1+A^2_2)],
\end{aligned} \tag{35}$$

while the correction terms in the extended version of the Euclidean Hamiltonian constraint given in Eq. (24), resulting from the gauge unfixing procedure, reduce to

$$\begin{aligned}
&-\frac{1}{\kappa}\int_\Sigma d^3x \frac{N}{\sqrt{\det(E)}}\left\{\frac{\mathcal{I}_A E^A_I \mathcal{I}_B E^{IB}}{(E^r_3)^2} + \epsilon^{IJ}\frac{E^A_I(\partial_B E^B_J)\mathcal{I}_A}{E^r_3} + \epsilon^{IJ}E^A_I \mathcal{I}_B \partial_A\left(\frac{E^B_J}{E^r_3}\right) - E^r_3 E^A_I \partial_A\left(\frac{\partial_B E^{IB}}{E^r_3}\right)\right\}\\
&= \frac{1}{\kappa}\int_\Sigma d^3x \frac{N}{\sqrt{\det(E)}} E^A_I \partial_A \partial_B E^{IB}\\
&= -\frac{1}{\kappa}\int_\Sigma d^3x \frac{N(x)\sin\theta}{\sqrt{((E^1)^2+(E^2)^2)E^r}}((E^1)^2+(E^2)^2).
\end{aligned} \tag{36}$$

We thus see that

$$H^E_{\rm sph}[N] = \tilde{H}^E[N], \tag{37}$$

as expected; namely, the role of the extra terms in the extended Euclidean Hamiltonian is to provide the contribution given by $\partial_\theta A^3_\varphi$ inside $F^3_{\theta\varphi}$ in $H^E_{\rm sph}[N]$, since this is the only term where a connection component not belonging to the reduced phase space appears.

For the spherically symmetric Lorentzian part of the Hamiltonian constraint given in Eq. (28), we have

$$H_L[N] = -2\frac{(1+\gamma^2)}{\kappa}\int_\Sigma d^3x \frac{N(x)}{\sqrt{\det(E)}}(E^A_I E^B_J K^I_{[A}K^J_{B]} + E^r_3 E^A_I K^3_r K^I_A)$$
$$= \frac{(1+\gamma^2)}{\kappa}\int_\Sigma d^3x \frac{N(x)\sin\theta}{\sqrt{E^r}}\sqrt{(E^1)^2+(E^2)^2}K^2, \tag{38}$$

where

$$K = \frac{R'}{\Lambda}\left(N^r - \frac{\dot{R}}{R'}\right) \tag{39}$$

is the trace of extrinsic curvature of Σ_t. Let us also write the Lorentzian Hamiltonian constraint in terms of the Ricci scalar. By means of Eq. (A17), we have

$$\begin{aligned}
H_L[N] &= -\frac{1}{\kappa}\left(1+\frac{1}{\gamma^2}\right)\int_\Sigma d^3x N(x)\sqrt{\det(E)}R \\
&= \frac{1}{\kappa}\left(1+\frac{1}{\gamma^2}\right)\int_\Sigma d^3x \frac{N(x)}{2(E^r_3)^{5/2}\sin^{1/2}\theta[(E^\varphi_1)^2+(E^\varphi_2)^2]^{3/2}}[-2\sin^2\theta(E^\varphi_1)^4[(\partial_\theta E^r_3)^2 - E^r_3\partial^2_\theta E^r_3] \\
&\quad - 2\sin\theta E^r_3(E^\varphi_1)^3[\partial_\theta E^r_3\partial_\theta E^\theta_2 + E^r_3\partial^2_\theta E^\theta_2] - 2E^r_3E^\varphi_1(E^\varphi_2[(\sin\theta E^\varphi_2\partial_\theta E^r_3 - 4E^r_3\partial_\theta E^\theta_1)\partial_\theta E^\theta_2 + \sin\theta E^r_3E^\varphi_2\partial^2_\theta E^\theta_2] \\
&\quad + 2(E^r_3)^2\partial_r E^\varphi_1\partial_r E^r_3) + (E^\varphi_1)^2(-4\sin^2\theta(E^\varphi_2)^2[(\partial_\theta E^r_3)^2 - E^r_3\partial^2_\theta E^r_3] + 2\sin\theta E^r_3E^\varphi_2[\partial_\theta E^r_3\partial_\theta E^\theta_1 + E^r_3\partial^2_\theta E^\theta_1] \\
&\quad + (E^r_3)^2[4(\partial_\theta E^\theta_1)^2 + (\partial_r E^r_3)^2 + 4E^r_3\partial^2_r E^r_3]) + E^\varphi_2(-2\sin^2\theta(E^\varphi_2)^3[(\partial_\theta E^r_3)^2 - E^r_3\partial^2_\theta E^r_3] + 2\sin\theta \\
&\quad \times E^r_3(E^\varphi_2)^2[\partial_\theta E^r_3\partial_\theta E^\theta_1 + E^r_3\partial^2_\theta E^\theta_1] - 4(E^r_3)^3\partial_r E^\varphi_2\partial_r E^r_3 + (E^r_3)^2E^\varphi_2[4(\partial_\theta E^\theta_2)^2 + (\partial_r E^r_3)^2 + 4E^r_3\partial^2_r E^r_3])] \\
&= -\frac{2}{\kappa}\left(1+\frac{1}{\gamma^2}\right)\int_\Sigma d^3x N(x)\sin\theta\left[\frac{2R}{\Lambda}\left(\frac{R'\Lambda'}{\Lambda} - R''\right) + \Lambda\left(1 - \frac{(R')^2}{\Lambda^2}\right)\right].
\end{aligned} \tag{40}$$

The expression in terms of the fluxes that appears in the second equality above is the one that we are going to use to quantize the Lorentzian Hamiltonian constraint. In fact, given the diagonal action of the reduced flux operators, we can compute its expectation value in a lengthy but straightforward manner, without having to rely on any recoupling theory. Despite the fact that we used spherical symmetry to arrive at this expression, such simplifications would in any case be enforced by the coherent states that we build in the next section. This way we have simplified the calculation of the expectation value of the Lorentzian Hamiltonian without the need to sacrifice any relevant quantum corrections (see Appendix A for more details on the symmetry assumptions used to derive the expression above).

IV. QUANTUM REDUCED LOOP GRAVITY KINEMATICAL HILBERT SPACE

In this section we construct step by step a reduced kinematical Hilbert space $\mathcal{H}^R$ that implements at the quantum level the radial partial gauge fixing in Eq. (21). We start with the standard LQG kinematical Hilbert space $\mathcal{H}^K$ representing quantum holonomy-flux algebra. We then perform a weak imposition for the quantum version of Eq. (21) that restricts the non-gauge-invariant spin network basis states arriving at $\mathcal{H}^R$. Symbolically, $P\mathcal{H}^K = \mathcal{H}^R$, where P is the projection operator defined below.

The first ingredient of the quantum reduction process consists of a choice of spatial manifold triangulation adapted to the topology of interest and selecting a subclass of graphs labeling the spin network basis of $\mathcal{H}^R$. A natural choice for a spherically symmetric geometry is to restrict to cuboidal triangulations, where at each vertex we have three directions, one corresponding to the radial direction and the other two to the angular directions on the 2-spheres foliating the spatial manifold.

In what follows we present the technical details of our construction.

A. Reduced spin network states

Given a two-dimensional surface S^a with normal vector

$$n_a = \frac{\partial x^b}{\partial\sigma_1}\frac{\partial x^c}{\partial\sigma_2}\epsilon_{abc}, \tag{41}$$

where σ_1 and σ_2 are local coordinates on S^a, we restrict our choice of fluxes to the surfaces whose normal vectors are aligned with the three tangent directions r, θ, φ. We choose two $su(2)$ orthonormal bases labeled by $\{x, y, z\}$ and $\{1, 2, 3\}$ for which the basis elements 3 and z coincide

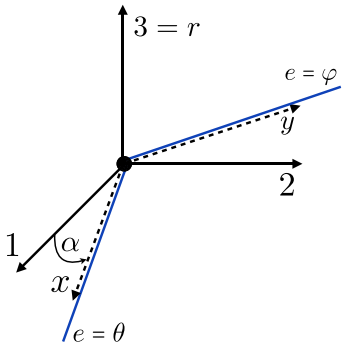

FIG. 1. Tangent and internal directions.

$[\{1,2\}$ differ from $\{x,y\}$ by an $SO(2)$ rotation $\alpha]$. Consistently with our classical gauge fixing, we take the direction r to be aligned with the internal direction 3 while the directions θ and φ are aligned with x and y (see Fig. 1). Therefore, our gauge fixing reads

$$E_3(S^\theta) = 0 = E_3(S^\varphi), \tag{42}$$

$$E_1(S^r) = 0 = E_2(S^r), \tag{43}$$

where

$$E_i(S^a) = \int E^a_i n_a d\sigma_1 d\sigma_2. \tag{44}$$

In order to implement the above partial gauge fixing at the quantum level, we select cuboidal graphs Γ's adapted to this set of coordinates. This means that the edges e are aligned with the three directions $\{r,\theta,\varphi\}$ such that $\dot{e}^a_e \propto \delta^a_e$. Along these directions the $SU(2)$ holonomies are

$$g_e = \mathcal{P} e^{\int_e \tau_i A^i_a \dot{e}^a_e(s) ds}. \tag{45}$$

The set of discretized 2-spheres at a given value of r is equipped with a grid of plaquettes with edges labeled by the tangential coordinates θ and φ. In a graphical representation, this is given by

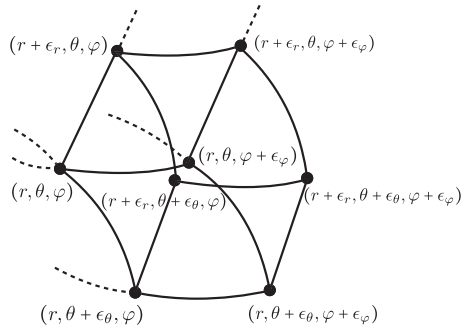

(46)

with ϵ_r, ϵ_θ, and ϵ_φ being coordinate lengths in the tangential directions. We designate this set as the set of reduced graphs. Our projection operator P acts on $\mathcal{H}^K = \oplus_\gamma \mathcal{H}^K_\gamma$, where γ are arbitrary graphs labeling $\mathcal{H}^K$, in two steps: first by restricting γ to Γ, where Γ is given by cubulation of at most 6-valent vertices as shown in Eq. (46), and then projecting $\mathcal{H}^K_\Gamma$ to its reduced subspace $\mathcal{H}^R_\Gamma$. The kinematical Hilbert space $\mathcal{H}^R$ is then obtained from the direct sum over all reduced graphs of this form that we construct from the union of Γ, namely

$$\mathcal{H}^R = \oplus_\Gamma \mathcal{H}^R_\Gamma. \tag{47}$$

$\mathcal{H}^R_\Gamma$ is defined by assigning to each link in a given tangent direction the following basis elements:

$${}^x D^{j_x}_{\bar{m}_x \bar{n}_x}(g_\theta) = \langle \bar{m}_x, \vec{u}_x | D^{j_x}(g_\theta) | \bar{n}_x, \vec{u}_x \rangle = \langle g_\theta | x, j_x, \tilde{m}_x, \tilde{n}_x \rangle, \tag{48a}$$

$${}^y D^{j_y}_{\bar{m}_y \bar{n}_y}(g_\varphi) = \langle \bar{m}_y, \vec{u}_y | D^{j_y}(g_\varphi) | \bar{n}_y, \vec{u}_y \rangle = \langle g_\varphi | y, j_y, \tilde{m}_y, \tilde{n}_y \rangle, \tag{48b}$$

$$D^{j_z}_{\bar{m}_z \bar{n}_z}(g_r) = \langle \bar{m}_z, j_z | D^{j_z}(g_r) | j_z, \bar{n}_z \rangle = \langle g_r | r, j_r, \tilde{m}_z, \tilde{n}_z \rangle, \tag{48c}$$

where $|j,m\rangle$ is an element of the spin basis that diagonalizes both $\tau^i \tau_i$ and τ_3, and $\bar{m}_x$, $\bar{n}_x = \pm j_x$, $\bar{m}_y$, $\bar{n}_y = \pm j_y$, and $\bar{m}_z$, $\bar{n}_z = \pm j_z$. We denote two orthogonal unit vectors in the arbitrary internal directions $I \in \{x,y\}$ on the (1,2)-plane by $\vec{u}_I$. Then

$$|\bar{n}_I, \vec{u}_I\rangle = D^{j_I}(\vec{u}_I) |j_I, \bar{n}_I\rangle = \sum_m |j_I, m\rangle D^{j_I}_{m\bar{n}_I}(u_I) \tag{49}$$

is an $SU(2)$ coherent state having maximum or minimum magnetic number along $\vec{u}_I$ [$D^j_{mn}(g)$ are the standard Wigner matrices in the spin basis $|j,m\rangle$].

The basis elements given in Eqs. (48) and (48) can also be written as

$${}^I D^{j_I}_{\bar{m}_I \bar{n}_I}(g) = D^{j_I - 1}_{\bar{m}_I m}(u_I) D^{j_I}_{mn}(g) D^{j_I}_{n\bar{n}_I}(u_I), \tag{50}$$

where u_I is an $SU(2)$ group element that rotates the 3-axis into $\vec{u}_I$ and repeated indices are summed over. Given the convention shown in Fig. 1, we parametrize the rotation group elements as

$$u_x = R\left(\alpha, \frac{\pi}{2}, 0\right) = e^{\alpha \tau_3} e^{\frac{\pi}{2}\tau_2}, \tag{51}$$

$$u_y = R\left(\alpha + \frac{\pi}{2}, \frac{\pi}{2}, -\frac{\pi}{2}\right) = e^{(\alpha + \frac{\pi}{2})\tau_3} e^{\frac{\pi}{2}\tau_2} e^{-\frac{\pi}{2}\tau_3}. \tag{52}$$

The angle α above that enters the construction of the reduced states and the operators that we construct

below is *a priori* independent of $\tilde{\alpha}$ that appears in the classical solutions for the connection and the densitized triad of Sec. II [the relation between the couples of internal directions (1,2) and (x, y) can be chosen independently for the classical solution and the quantum construction]. In order to implement the residual $U(1)$ gauge invariance, we are going to integrate over the angle α in the reduced states, while the $\tilde{\alpha}$ appearing in the classical solutions given in Eqs. (12) and (13) for triad and connection, around which our semiclassical states are peaked, is held fixed.

Notice that unlike the reduced states built for cosmological applications in [86], in Eq. (48) we also include the off-diagonal terms, i.e., states peaked on maximum-minimum magnetic numbers and not just maximum-maximum or minimum-minimum. As we will show below, these states are in fact allowed by the radial gauge fixing given in Eq. (21). They are important in the black hole context since the symmetry reduced Ashtekar-Barbero connection contains general off-diagonal terms (see Sec. III A).

We can now show that on $\mathcal{H}^R$ the gauge fixing conditions given in Eqs. (42) and (43) are weakly satisfied. Let us concentrate on 3-cells with surfaces S^a that intersect the respective dual edges $\dot{e}^a_e$ only once. Hence S^a are three orthogonal faces of the cube dual to a 6-valent node of the reduced graph. This provides a regularization of the reduced fluxes. By means of the Baker-Hausdorff formula, let us first derive the following relations:

$$u_x\tau_3 u_x^{-1} = \tau_1\cos\alpha + \tau_2\sin\alpha = \tau_x, \tag{53a}$$

$$u_y\tau_3 u_y^{-1} = -\tau_1\sin\alpha + \tau_2\cos\alpha = \tau_y, \tag{53b}$$

$$u_x^{-1}\tau_3 u_x = \tau_1, \tag{53c}$$

$$u_y^{-1}\tau_3 u_y = -\tau_2, \tag{53d}$$

$$u_x^{-1}\tau_1 u_x = \tau_3\cos\alpha - \tau_2\sin\alpha, \tag{53e}$$

$$u_y^{-1}\tau_1 u_y = -\tau_3\sin\alpha + \tau_1\cos\alpha, \tag{53f}$$

$$u_x^{-1}\tau_2 u_x = \tau_3\sin\alpha + \tau_2\cos\alpha, \tag{53g}$$

$$u_y^{-1}\tau_2 u_y = \tau_3\cos\alpha + \tau_1\sin\alpha. \tag{53h}$$

It is then immediate that

$$\begin{aligned}&\langle j'_x, \bar{m}'_x, \bar{n}'_x, x|\hat{E}_3(S^\theta)|x, j_x, \bar{m}_x, \bar{n}_x\rangle \\ &\quad= -i\kappa\gamma o(\ell_3, S^\theta)\int dg\,\overline{{}^x D^{j'_x}_{\bar{m}'_x\bar{n}'_x}(g)}\,{}^x D^{j_x}_{\bar{m}_x m}(\tau_3)\,{}^x D^{j_x}_{m\bar{n}_x}(g) \\ &\quad= -i\kappa\gamma o(\ell_3, S^\theta)\,{}^x D^{j_x}_{\bar{m}_x\bar{m}_x}(\tau_3) = 0,\end{aligned} \tag{54}$$

and similarly for the other gauge fixing conditions. Notice that this relation is only valid for $j \neq 1/2$ since in that case the off-diagonal matrix elements will not be necessarily vanishing. However, this case is not relevant for our construction because we are only interested in the semiclassical limit of the effective Hamiltonian through coherent states which provide good approximation to classical geometry only in the limit $j \gg 1$ (see Sec. VI). Since these states peak the spin quantum numbers on large values, the spin $1/2$ contributions to the semiclassical expectation values we compute below are largely suppressed and we do not have to worry about them for the purposes of our analysis.

For the other components of the fluxes which are classically nonvanishing we get the following expectation values:

$$\begin{aligned}\langle\hat{E}_3(S^r)\rangle &= -i\kappa\gamma o(\ell_3, S^r) D^{j_z}_{\bar{m}_z\bar{m}_z}(\tau_3) \\ &= -\kappa\gamma o(\ell_3, S^r)\bar{m}_z,\end{aligned} \tag{55a}$$

$$\begin{aligned}\langle\hat{E}_1(S^\theta)\rangle &= -i\kappa\gamma o(\ell_x, S^\theta)\,{}^x D^{j_x}_{\bar{m}_x\bar{m}_x}(\tau_1) \\ &= -\kappa\gamma o(\ell_x, S^\theta)\bar{m}_x\cos\alpha,\end{aligned} \tag{55b}$$

$$\begin{aligned}\langle\hat{E}_1(S^\varphi)\rangle &= -i\kappa\gamma o(\ell_y, S^\varphi)\,{}^y D^{j_y}_{\bar{m}_y\bar{m}_y}(\tau_1) \\ &= \kappa\gamma o(\ell_y, S^\varphi)\bar{m}_y\sin\alpha,\end{aligned} \tag{55c}$$

$$\begin{aligned}\langle\hat{E}_2(S^\theta)\rangle &= -i\kappa\gamma o(\ell_x, S^\theta)\,{}^x D^{j_x}_{\bar{m}_x\bar{m}_x}(\tau_2) \\ &= -\kappa\gamma o(\ell_x, S^\theta)\bar{m}_x\sin\alpha,\end{aligned} \tag{55d}$$

$$\begin{aligned}\langle\hat{E}_2(S^\varphi)\rangle &= -i\kappa\gamma o(\ell_y, S^\varphi)\,{}^y D^{j_y}_{\bar{m}_y\bar{m}_y}(\tau_2) \\ &= -\kappa\gamma o(\ell_y, S^\varphi)\bar{m}_y\cos\alpha,\end{aligned} \tag{55e}$$

where $o(\ell, S)$ is a sign denoting the orientation between a link and its dual face. All off-diagonal matrix elements vanish for these operators as well, as long as $j \neq 1/2$, which, as just explained, is not relevant for the semiclassical limit.

B. Quantum Gauss constraint

We proceed by projecting the kernel of the full theory Gauss constraint. As expected, this will be performed by the operation

$$P^\dagger\hat{G}_i P, \tag{56}$$

where P is the projection operator defined previously. The kernel of $\hat{G}_i$ is given by the well-known gauge-invariant spin network states obtained by contraction with the $SU(2)$ intertwiners at the nodes of the graphs. Operator P is then restricting the intertwiners in the way explained in Sec. IV C. The operation $P^\dagger\hat{G}_i P$ maps the kernel of $\hat{G}_i$ to

the kernel of ${}^R\hat{G}_3$, representing the classical phase space reduction given in Eq. (22). The states annihilated by ${}^R\hat{G}_3$ are now α invariant, where α is parameter of rotation around the internal 3-axis that has been aligned to the r-axis by the projector P.

C. 3-valent vertex state

Let us write the resolution of the identity in terms of coherent states:

$$\begin{aligned}\mathbb{I}_j &= \sum_m |j,m\rangle\langle m,j| \\ &= d_j \int_{S^2} d\vec{u}\,|\bar{m},\vec{u}\rangle\langle\vec{u},\bar{m}| \\ &= d_j \sum_{m,n} \int_{S^2} d\vec{u} D^j_{m\bar{m}}(u)\overline{D^j_{n\bar{m}}(u)}|j,m\rangle\langle n,j|. \end{aligned} \tag{57}$$

The gauge-invariant version of our states given in Eq. (50) can be obtained from the standard gauge-invariant spin network states as

$$\begin{aligned}\iota^{*m}_{j_I} D^{j_I}_{mn}(g)\iota^n_{j_I} &= d^2_{j_I}\int_{S^2} du^1_I du^2_I \iota^{*m}_{j_I}\langle m,j_I|\bar{m}_I,\vec{u}^1_I\rangle\langle\vec{u}^1_I,\bar{m}_I|D^{j_I}(g)|\bar{n}_I,\vec{u}^2_I\rangle\langle\vec{u}^2_I,\bar{n}_I|j_I,n\rangle\iota^n_{j_I} \\ &= d^2_{j_I}\sum_{a,b,c,d}\int_{S^2} du^1_I du^2_I \iota^{*m}_{j_I} D^{j_I}_{a\bar{m}_I}(u^1_I)\overline{D^{j_I}_{b\bar{m}_I}(u^1_I)}\langle m,j_I|j_I,a\rangle\langle b,j_I|D^{j_I}(g)|j_I,c\rangle\langle d,j_I|j_I,n\rangle D^{j_I}_{c\bar{n}_I}(u^2_I)\overline{D^{j_I}_{d\bar{n}_I}(u^2_I)}\iota^n_{j_I} \\ &= d^2_{j_I}\int_{S^2} du^1_I du^2_I \iota^{*m}_{j_I} D^{j_I}_{m\bar{m}_I}(u^1_I) D^{j_I}_{\bar{m}_I\bar{n}_I}((u^1_I)^{-1}gu^2_I)\overline{D^{j_I}_{n\bar{n}_I}(u^2_I)}\iota^n_{j_I} \end{aligned} \tag{58}$$

where $\iota^{*m}_{j_I}$ is an intertwiner in the 3 basis. Setting $u^1_I = u^2_I = u_I$ amounts to projection on $\mathcal{H}^R$. The reduced holonomies are then obtained by restricting the Haar measure du only to $U(1)$ rotation around the z-axis, namely

$$\begin{aligned}{}^R D^{j_I}_{mn}(g) = d^2_{j_I}\int_0^{2\pi} d\alpha D^{j_I}_{m\bar{m}_I}(u_I(\alpha)) \\ \times D^{j_I}_{\bar{m}_I\bar{n}_I}((u_I(\alpha))^{-1}gu_I(\alpha))\overline{D^{j_I}_{n\bar{n}_I}(u_I(\alpha))}. \end{aligned} \tag{59}$$

In a graphical notation, this is

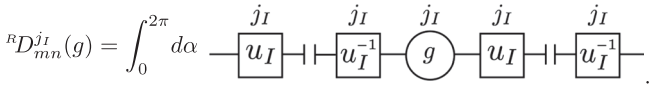

(60)

Here we denoted the projection on the highest or lowest magnetic number as

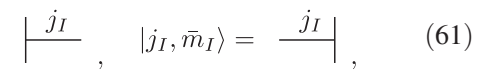

(61)

and the Wigner matrices in the $|j,m\rangle$ basis for the u_I rotations and a generic $SU(2)$ group element g respectively as

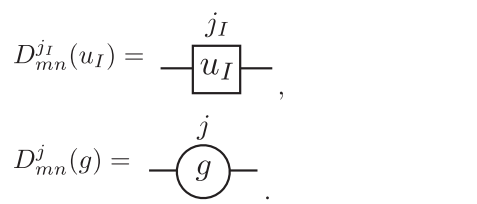

Using this notation, we can represent a reduced 3-valent vertex state as

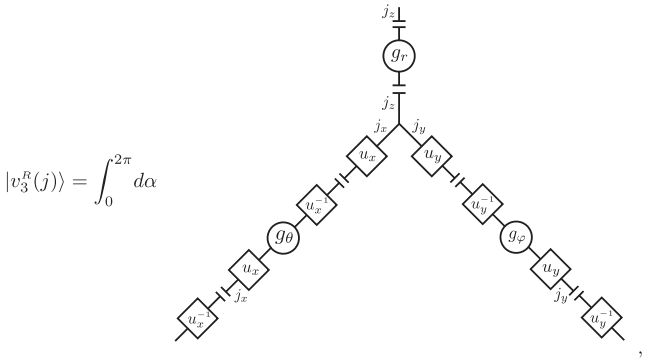

(62)

where the 3-valent node represents the standard $3-j$ symbol and its contraction with $SU(2)$ coherent states defines the reduced intertwiners.

D. Geometric operators

On $\mathcal{H}^R$ that we constructed above, we can now define the action of geometric operators such as the area and the volume operators by importing the regularization techniques of the full theory [109–111]. These geometric operators are constructed out of the reduced flux operators defined as follows. Let us introduce the projectors

$$\hat{P}^z = \sum_{\bar{m}_z=\pm j_z} |j_z,\bar{m}_z\rangle\langle\bar{m}_z,j_z|, \tag{63}$$

$$\hat{P}^I = \sum_{\bar{m}_I = \pm j_I} |\vec{u}_I, \bar{m}_I\rangle\langle \bar{m}_I, \vec{u}_I|, \tag{64}$$

where we recall $I \in \{x, y\}$. The reduced flux operators are then

$${}^R\hat{E}_i(S^r) = \hat{P}^z \hat{E}_i(S^r)\hat{P}^z, \tag{65}$$

$${}^R\hat{E}_i(S^\theta) = \hat{P}^x \hat{E}_i(S^\theta)\hat{P}^x, \tag{66}$$

$${}^R\hat{E}_i(S^\varphi) = \hat{P}^y \hat{E}_i(S^\varphi)\hat{P}^y. \tag{67}$$

In a similar fashion as one can prove the validity of the partial gauge fixing condition given in Eq. (54) (as well as all the others), it is immediate to see that the reduced flux operators defined above are diagonal on the reduced quantum states constructed in the previous part of this section. Nonvanishing eigenvalues correspond only to those components associated to the remaining reduced phase space densitized triad variables as written in Eq. (12), and they are given by the relations that appear in Eq. (55). This is a key result of our construction, which will allow us to compute the expectation value of the Hamiltonian constraint in a relatively straightforward manner. But let us first exploit this property of the reduced fluxes to compute the spectrum of the main geometrical operators in LQG.

We can concentrate on a 3-valent node with three links departing along the three directions $\{r, \theta, \varphi\}$ that appears in Eq. (62). If we consider three surfaces S^a that intersect the dual links ℓ_a once, we can construct the associated area operators in terms of the reduced fluxes given in Eqs. (65)–(67). The action of these reduced area operators on the reduced states associated with the dual links that they intersect is

$$\begin{aligned} {}^R\hat{A}(S^\theta){}^R D^{j_x}_{mn}(g_\theta) &= \sqrt{{}^R\hat{E}_i(S^\theta){}^R\hat{E}^i(S^\theta)}\,{}^R D^{j_x}_{mn}(g_\theta) \\ &= \kappa\gamma j_x {}^R D^{j_x}_{mn}(g_\theta), \end{aligned} \tag{68}$$

$$\begin{aligned} {}^R\hat{A}(S^\varphi){}^R D^{j_y}_{mn}(g_\varphi) &= \sqrt{{}^R\hat{E}_i(S^\varphi){}^R\hat{E}^i(S^\varphi)}\,{}^R D^{j_y}_{mn}(g_\varphi) \\ &= \kappa\gamma j_y {}^R D^{j_y}_{mn}(g_\varphi), \end{aligned} \tag{69}$$

$$\begin{aligned} {}^R\hat{A}(S^r){}^R D^{j_z}_{mn}(g_r) &= \sqrt{{}^R\hat{E}_i(S^r){}^R\hat{E}^i(S^r)}\,{}^R D^{j_z}_{mn}(g_r) \\ &= \kappa\gamma j_z {}^R D^{j_z}_{mn}(g_r). \end{aligned} \tag{70}$$

Next, we can consider the volume of the region containing only the 3-valent node v. The associated reduced volume operator regularized on the cube dual to v acts diagonally on the reduced 3-valent vertex state given in Eq. (62) as

$$\begin{aligned} &{}^R\hat{V}(v)|v_3^R(j)\rangle \\ &= \sqrt{\left|\frac{1}{3!}\epsilon_{abc}\epsilon^{ijk}{}^R\hat{E}_i(S^a){}^R\hat{E}_j(S^b){}^R\hat{E}_j(S^c)\right|}|v_3^R(j)\rangle \\ &= \sqrt{|({}^R\hat{E}_1(S^\theta){}^R\hat{E}_2(S^\varphi) - {}^R\hat{E}_2(S^\theta){}^R\hat{E}_1(S^\varphi)){}^R\hat{E}_3(S^r)|}|v_3^R(j)\rangle \\ &= (\kappa\gamma)^{\frac{3}{2}}\sqrt{|j_x j_y j_z|}|v_3^R(j)\rangle. \end{aligned} \tag{71}$$

This diagonal action of the volume operator on the reduced 3-valent vertex state represents a key characteristic of this construction which enables us to considerably simplify the calculation of the Hamiltonian constraint action.

E. Recoupling theory

In order to study the action of holonomy operators in $\mathcal{H}^R$, we need to define the recoupling theory for our states. To this end, for a product of states along the same direction we introduce the following "reduced" recoupling rule:

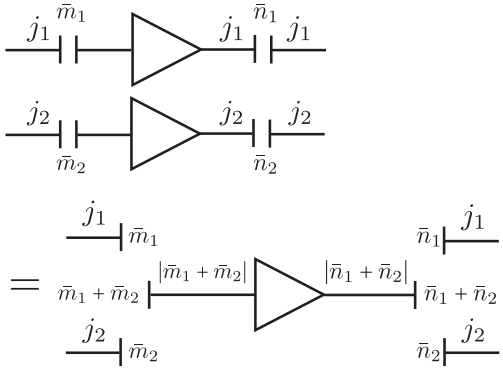

(72)

where a triangle denotes the Wigner matrix of either a given rotation or a generic $SU(2)$ element. Let us point out that in the case $\mathrm{sign}(\bar{m}_1\bar{m}_2) = \mathrm{sign}(\bar{n}_1\bar{n}_2) = +$, the explicit expression of the two Clebsch-Gordan coefficients $C^{Kk}_{j_1\bar{m}_1, j_2\bar{m}_2}$ and $C^{Kk}_{j_1\bar{n}_1, j_2\bar{n}_2}$ are nonvanishing only for $K = |\bar{m}_1 + \bar{m}_2|$, $k = \bar{m}_1 + \bar{m}_2$ and $K = |\bar{n}_1 + \bar{n}_2|$, $k = \bar{n}_1 + \bar{n}_2$ respectively. Hence, in this case the reduction is naturally implemented in this product rule. However, in the case where the two magnetic numbers have opposite signs, there is a tower of spins K that are allowed. In this case we need to restrict to the lowest spin in the tower in order for the reduction to be implemented in our recoupling rule. Moreover, in the case where the reduced states in the tensor product contain a $U(1)$ integral, as in Eq. (60), we first need to align the two states by fixing the same value for the $U(1)$ angles and then project by integrating the tensor product of the two states over this angle, in order to rewrite the product in terms of original reduced states on the links. We can now use these recoupling rules to compute the product of two 3-valent reduced states. Doing this we find

$$|v_3^R(j)\rangle \otimes |v_3^R(j')\rangle = \int_0^{2\pi} d\alpha$$

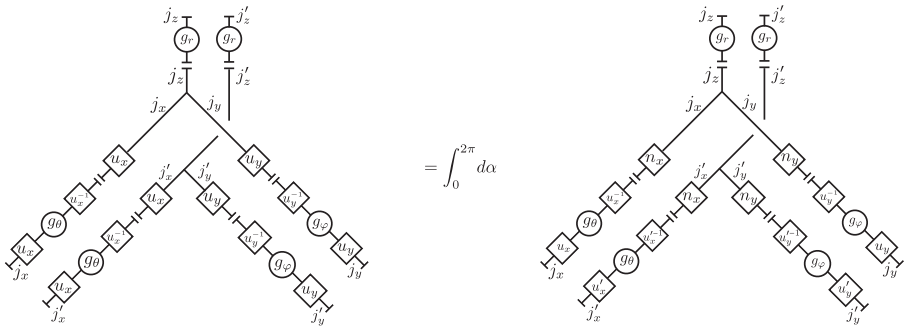

$$= \int_0^{2\pi} d\alpha$$

(73)

$$= \int_0^{2\pi} d\alpha$$

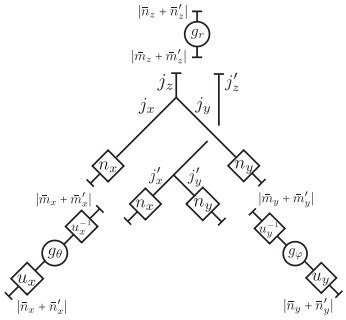

,

where we have introduced the graphical notation

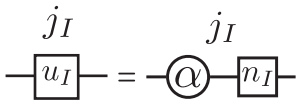

(74)

to use the fact that, due to the gauge invariance at the 3-valent node of $|v_3^R(j')\rangle$, the α dependence of the rotation group elements u_x, u_y [see Eqs. (51) and (52)] acting near the node can be reabsorbed and then the integral sees only these group elements on the links of the reduced state.

Finally, we can rewrite the product of two 3-valent reduced states as

$$|v_3^R(j)\rangle \otimes |v_3^R(j')\rangle = \begin{Bmatrix} j_x & j'_x & |\bar{m}_x + \bar{m}'_x| \\ j_y & j'_y & |\bar{m}_y + \bar{m}'_y| \\ j_z & j'_z & |\bar{m}_z + \bar{m}'_z| \end{Bmatrix} \int_0^{2\pi} d\alpha$$

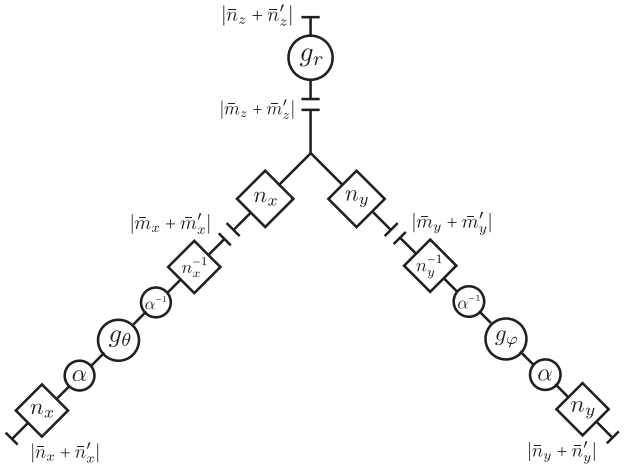

,

(75)

where we have used once more the recoupling rule of Eq. (72), as well as the standard $SU(2)$ recoupling theory, to rewrite the product in terms of an original reduced 3-valent vertex state times a $9j$ symbol.

If we now compute the norm of the 3-valent vertex state (62) through a scalar product consistent with the reduced recoupling rule introduced above, namely by again first aligning the bra and ket states, then performing the integration over the $SU(2)$ group elements through standard recoupling theory and finally performing the integral over α, we get

$$|v_3^R(j)| \equiv \sqrt{|\langle v_3^R(j)|v_3^R(j)\rangle|} = (2\pi)^{1/8}\sqrt{\left(\right)^{*}}$$

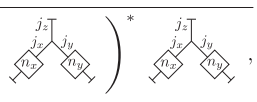

(76)

where the factor of $1/8$ for the 2π coming from the integral over α is due to the fact that the same angle α is eventually shared by four 3-valent vertices around a cell in the (x, y)-plane; similarly for $v_3^R(j')$. Therefore, comparing (73) with (75), we see that

$$|v_3^R(j)||v_3^R(j')| = (2\pi)^{1/8}\{9j\}|v_3^R(|\bar{m}+\bar{m}'|)|, \quad (77)$$

where the $9j$ symbol is the one in (75). It follows that, in terms of normalized 3-valent vertex states

$$|\widetilde{v_3^R}(j)\rangle = \frac{|v_3^R(j)\rangle}{|v_3^R(j)|}, \quad (78)$$

we get the product rule

$$|\widetilde{v_3^R}(j)\rangle \otimes |\widetilde{v_3^R}(j')\rangle = \frac{1}{(2\pi)^{1/8}}|\widetilde{v_3^R}(|\bar{m}+\bar{m}'|)\rangle. \quad (79)$$

Namely, by working with normalized intertwiners, the $9j$ symbol gets reabsorbed in the product rule and this provides a great simplification in the expectation value of the Hamiltonian constraint that we compute below.

Within this construction, the kinematical Hilbert space encodes the information of a radial metric tensor [as defined by the partial gauge fixing in Eqs. (42) and (43)]. The residual gauge freedom left is encoded by the $U(1)$ internal rotations around the 3-direction and radial diffeomorphisms preserving the reduced graphs structure, in accordance with the classical analysis of [97]. The latter can be implemented by standard group averaging techniques, defining the dual Hilbert space in terms of a sum over all the reduced graphs related by a (reduced) radial diffeomorphism with a shift smearing function depending only on the r coordinate.

F. Quantum vector constraint

The quantum vector constraint is imposed in the full theory by group averaging the spin network states over spatial diffeomorphisms as described in the seminal paper [112]. One introduces a Gelfand triple $\mathrm{Cyl} \subset \mathcal{H}^K \subset \mathrm{Cyl}^*$ where Cyl is the space of cylindrical functions. The vector constraint has a well-defined action on Cyl^*. Let $\mathcal{U}[\phi]$ be an operator acting on Cyl with ϕ being a self-diffeomorphism of Σ_t. We then have

$$\mathcal{U}[\phi]\psi_\gamma(A) = \psi_{\phi^{-1}\gamma}(A), \quad (80)$$

where $\psi_\gamma \in \mathrm{Cyl}$ and A is the Ashtekar-Barbero connection. However, since $\mathcal{U}[\phi]$ is not weakly continuous, it cannot be produced by a self-adjoint infinitesimal generator. Therefore one has to restrict attention to finite spatial diffeomorphisms when searching for diffeomorphism invariant states. Solving the "finite version" of the vector constraint equation boils down to searching for all ψ that satisfy

$$\mathcal{U}[\phi]\psi = \psi. \quad (81)$$

This equation, however, has no nontrivial solutions in $\mathcal{H}^K$. Nonetheless, it can be solved for $\psi \in \mathrm{Cyl}^*$. Formally, the solution is given as the averaging of the dual states over the group of spatial diffeomorphisms,

$$(\psi_{[\gamma]}| = \sum_{\phi\in \mathrm{Diff}(\Sigma_t)} \langle \psi_{\phi\gamma}|, \quad (82)$$

where $[\gamma]$ is the equivalence class of graphs.

In principle one should try to find the kernel of $\hat{\tilde{H}}_r$. But this goal is too ambitious at the moment. However, we know that classically and in the case where the shift vector N^r does not depend on the angular coordinates [see Eq. (23)], $\tilde{H}_r = {}^R\tilde{H}_r$. Therefore it may not be implausible to assume that the kernels of the corresponding quantized operators coincide. We expect that averaging the kinematical states constructed here over the group of radial diffeomorphisms will provide the required solutions to Eq. (81).

V. REDUCED HAMILTONIAN CONSTRAINT OPERATOR

A regularized expression of the Hamiltonian constraint operator in LQG was introduced in [105] with an action defined on a graph-dependent triangulation of the spacelike hypersurfaces. This construction can be easily adapted to the cubulation used here to define $\mathcal{H}^R$.

A. Euclidean term

Importing techniques developed for the cosmological case [84,88], we can define the Euclidean part of the reduced Hamiltonian constraint regularized on the faces of a cubic cell dual to a 6-valent node v (modulo an overall constant) as

$${}^R\hat{H}^E_\square[N] = -\frac{2}{\kappa^2\gamma}N(v)\epsilon^{ijk}\mathrm{Tr}[({}^R\hat{g}_{\alpha_{ij}} - {}^R\hat{g}^{-1}_{\alpha_{ij}}){}^R\hat{g}^{-1}_{s_k}[{}^R\hat{g}_{s_k}, {}^R\hat{V}(v)]], \quad (83)$$

where $N(v)$ is the lapse function at the node v; the reduced holonomies ${}^R\hat{g}$ are taken in the fundamental representation; and the internal indices i, j, k take values over $3, x, y$. In the regularization above, the link s_k corresponds to one of the six edges ℓ_3, ℓ_x, ℓ_y (two per direction, both denoted with

the same ℓ_i) departing from the node v, while α_{ij} corresponds to a loop in the plane (ij). Thus $\alpha_{ij} = \ell_i \circ \ell_j \circ \ell_i^{-1} \circ \ell_j^{-1}$ and we consider the non-graph-changing version of Thiemann's regularization. We take the Hamiltonian operator in the fundamental representation.

To elucidate the action of the operator given in Eq. (83), it is enough to concentrate on a reduced 3-valent vertex state that is defined in Eq. (62) for the case $k = z$, $i = x$, $j = y$. The other components of Eq. (83) act in a similar fashion. The extra structure of the 6-valent vertex state, namely the 6-valent reduced intertwiner, is not directly affected by the action of ${}^R\hat{H}^E_\square[N]$. In fact, in the process of computing the expectation value of ${}^R\hat{H}^E_\square[N]$ those coefficients cancel due to normalization. By means of the reduced recoupling rules introduced in Sec. IV E, the reduced Hamiltonian constraint action can be computed analogously to the cosmological case [86] and it yields

$$-\frac{2}{\kappa^2\gamma} N(v) \mathrm{Tr}\left[\left({}^R\hat{g}_{\alpha_{xy}} - {}^R\hat{g}^{-1}_{\alpha_{xy}}\right) {}^R\hat{g}^{-1}_{s_z} [{}^R\hat{g}_{s_z}, {}^R\hat{V}(v)]\right] |v_3^R(j)\rangle$$

$$= -4\pi\sqrt{\frac{\gamma}{\kappa}} N(v) \sum_{\mu=\pm 1/2} s(\mu)\sqrt{j_x j_y (j_z+\mu)} \int_0^{2\pi} d\alpha$$

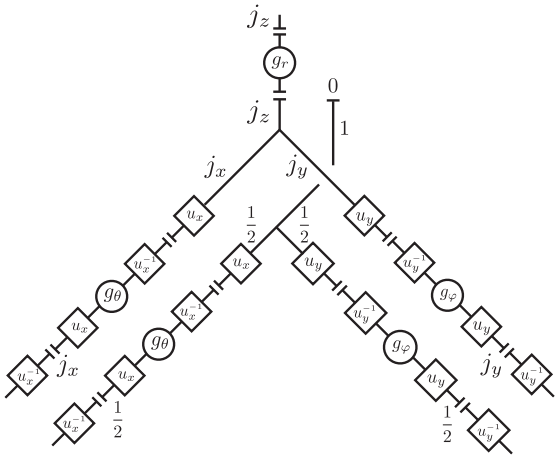

$$= -4\pi\sqrt{\frac{\gamma}{\kappa}} N(v) \sum_{\mu,\mu_x^m,\mu_x^n,\mu_y^m,\mu_y^n=\pm 1/2} s(\mu)\sqrt{j_x j_y (j_z+\mu)} \int_0^{2\pi} d\alpha$$

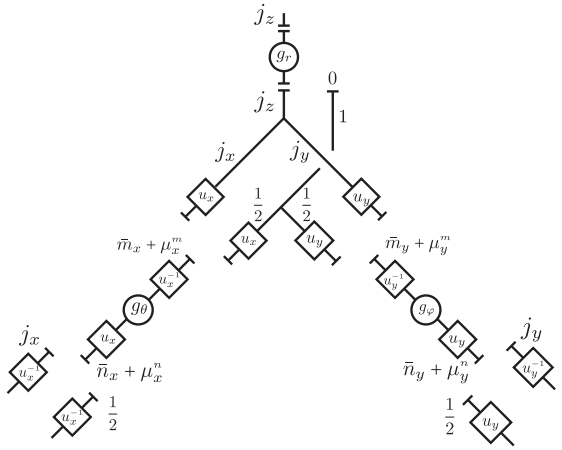

(84)

If we now include also the other three 3-valent nodes of the graph that close the loop attached by the Hamiltonian constraint and we denote the associated state as $|v^R_\square\rangle$, we obtain

$$-\frac{2}{\kappa^2\gamma}N(v)\mathrm{Tr}\left[\left({}^R\hat{g}_{\alpha_{xy}}-{}^R\hat{g}^{-1}_{\alpha_{xy}}\right){}^R\hat{g}^{-1}_{s_z}[{}^R\hat{g}_{s_z},{}^R\hat{V}(v)]\right]|v^R_\square\rangle$$

$$=-4\pi\sqrt{\frac{\gamma}{\kappa}}N(v)\sum_{\mu,\mu^m_x,\mu^n_x,\mu^m_y,\mu^n_y,\mu^{m'}_x,\mu^{n'}_x,\mu^{m'}_y,\mu^{n'}_y=\pm1/2}s(\mu)\sqrt{j_xj_y(j_z+\mu)}\int_0^{2\pi}d\alpha \tag{85}$$

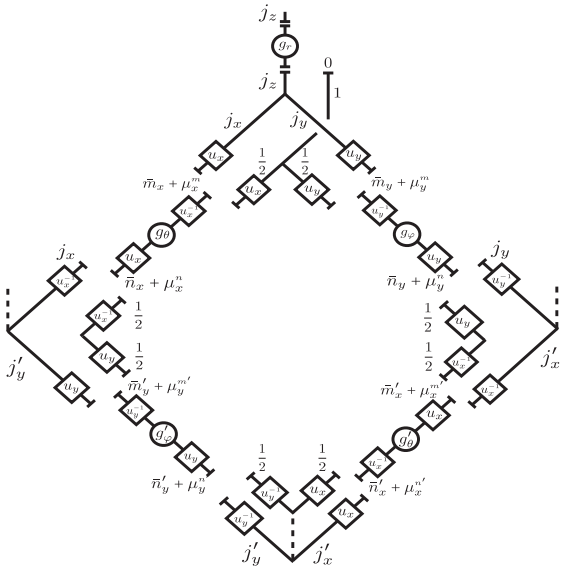

where $s(\mu)$ denotes the sign of μ and the dashed lines indicate the radial links of the other nodes where the constraint has not acted. Notice that we have not used the recoupling theory at the nodes since, in the expectation value of the Hamiltonian constraint, the intertwiners of the states will get reabsorbed in the normalization of the vertices [see Eq. (76)].

The complete action of the operator given in Eq. (83) can now be deduced from Eq. (84) with the following consideration. The loop operator in the ij plane, being made of ${}^iD$ and ${}^jD$ reduced states, will introduce the 2-valent intertwiners projected in the ij direction and a coupling of the spins. The expression ${}^R\hat{g}^{-1}_{s_k}[{}^R\hat{g}_{s_k},{}^R\hat{V}(v)]$ will now just introduce a 3-valent intertwiner oriented along ijk and a coefficient $\sqrt{j_ij_j(j_k+1/2)}-\sqrt{j_ij_j(j_k-1/2)}$. The resulting expression is given by the sum over cyclic permutations of the second line of Eq. (85).

B. Lorentzian term

As anticipated above, we are going to quantize the Lorentzian term of the Hamiltonian constraint starting from its classical expression in terms of the Ricci scalar as it appears in Eq. (31). In fact, by replacing the spin connection components in terms of the fluxes and their first and second derivatives, as follows from solving the torsion-free condition, we obtain the Lorentzian term in the form given in Eq. (40). In the final operator only the reduced fluxes and their derivatives appear. In the $\mathcal{H}^R$ construction that was outlined in Sec. IV D, we saw how the reduced fluxes have a representation which is diagonal on the reduced spin network states. The spatial derivatives of the reduced fluxes ${}^RE_i(S^b(x))$ can be quantized in terms of discrete differences of reduced flux operators acting on neighboring links. More precisely, for first and second order derivatives we have, respectively,

$$\partial_a{}^R\hat{E}_i(S^b(v))\equiv{}^R\hat{E}_i(S^b(v+\epsilon_a))-{}^R\hat{E}_i(S^b(v)), \tag{86}$$

$$\partial^2_a{}^R\hat{E}_i(S^b(v))\equiv{}^R\hat{E}_i(S^b(v+2\epsilon_a))-2{}^R\hat{E}_i(S^b(v+\epsilon_a))+{}^R\hat{E}_i(S^b(v)), \tag{87}$$

where v denotes the node whose departing links are dual to the surfaces S^b where the fluxes are smeared and $v+\epsilon_a(v+2\epsilon_a)$ are the neighboring (next to the neighboring) nodes in the direction a, taking into account the spatial manifold orientation.

In this way, the lengthy expression in Eq. (40) can be quantized in a straightforward manner, without having to rely on Thiemann's regularization techniques [105] for the Lorentzian term expressed in terms of the extrinsic curvature. We will use the quantization scheme given in Eqs. (86) and (87) to compute the expectation value of the Lorentzian Hamiltonian operator in Sec. VII B below (as well as for the extension term of the Euclidean part in Sec. VII A). See Appendix C for an alternative quantization scheme for the 3D Ricci scalar.

VI. SEMICLASSICAL STATES

The construction of semiclassical states in $\mathcal{H}^R$ follows the prescription outlined in [86], which is in turn based on the definition introduced in [113].[11] The key ingredient is the heat kernel of the Laplace operator for each edge ℓ of the graph acting on the δ-function of the $SU(2)$ group element g_ℓ associated to the link. Explicitly

$$K_\lambda(g_\ell, g) = e^{-\frac{\lambda}{2}\Delta_{g_\ell}}\delta(g_\ell, g) = \sum_{j_\ell}(2j_\ell+1)e^{-\frac{\lambda}{2}j_\ell(j_\ell+1)}\chi_{j_\ell}(g_\ell^{-1}g), \tag{88}$$

with λ being a positive real number controlling the fluctuations of the state and χ_{j_ℓ} the $SU(2)$ character in the irreducible representation j_ℓ. Here we are introducing the convention that the index ℓ indicates both the tangent coordinate and the associated internal direction, namely $\ell \in \{(r,z),(\theta,x),(\varphi,y)\}$. Coherent semiclassical states are then obtained by analytic continuation from $g \in SU(2)$ to $G \in SL(2,\mathbb{C})$, namely

$$\psi^\lambda_G(g_\ell) = K_\lambda(g_\ell, G), \tag{89}$$

where the complexifier G reads

$$G = g\exp\left(i\frac{\lambda}{\kappa\gamma}E_i(S^\ell)\tau^i\right), \tag{90}$$

and $E_i(S^\ell)$ is the flux across the surface dual to the link ℓ of area δ_ℓ^2 in the fiducial metric.

Therefore, using the classical expressions for the fluxes and connection components found in the previous sections, the semiclassical states for the three directions of the cellular decomposition read (see Appendix B for more details on the derivation)

$$\begin{aligned}\psi^\lambda_G(g_r) &= \sum_{j_z=0}^{\infty}\sum_{\tilde m_z,\tilde n_z}(2j_z+1)e^{-\frac{\lambda}{2}j_z(j_z+1)}D^{j_z}_{\tilde m_z\tilde n_z}(g_r^{-1})D^{j_z}_{\tilde n_z\tilde m_z}(e^{\epsilon_r A_r\tau_3}e^{i\frac{\lambda\delta_r^2}{\kappa\gamma}E^r\sin\theta\tau_3})\\ &= \sum_{j_z=0}^{\infty}\sum_{\tilde m_z}(2j_z+1)e^{-\frac{\lambda}{2}j_z(j_z+1)}e^{\lambda\tilde m_z\frac{\delta_r^2E^r\sin\theta}{\kappa\gamma}}D^{j_z}_{\tilde n_z\tilde m_z}(e^{\epsilon_r A_r\tau_3})D^{j_z}_{\tilde m_z\tilde n_z}(g_r^{-1}),\end{aligned} \tag{91}$$

$$\begin{aligned}\psi^\lambda_G(g_\theta) &= \sum_{j_x=0}^{\infty}\sum_{\tilde m_x,\tilde n_x}(2j_x+1)e^{-\frac{\lambda}{2}j_x(j_x+1)x}D^{j_x}_{\tilde m_x\tilde n_x}(g_\theta^{-1})^xD^{j_x}_{\tilde n_x\tilde m_x}(e^{\epsilon_\theta(A_1\tau_1+A_2\tau_2)}e^{i\frac{\lambda\delta_\theta^2}{\kappa\gamma}(E^1\tau_1+E^2\tau_2)\sin\theta})\\ &= \sum_{j_x=0}^{\infty}\sum_{\tilde m_x,\tilde n_x}(2j_x+1)e^{-\frac{\lambda}{2}j_x(j_x+1)}e^{\lambda\tilde m_x\frac{\delta_\theta^2E^x}{\kappa\gamma}x}D^{j_x}_{\tilde n_x\tilde m_x}(e^{\epsilon_\theta(A_1\tau_1+A_2\tau_2)})^xD^{j_x}_{\tilde m_x\tilde n_x}(g_\theta^{-1}),\end{aligned} \tag{92}$$

$$\begin{aligned}\psi^\lambda_G(g_\varphi) &= \sum_{j_y=0}^{\infty}\sum_{\tilde m_y,\tilde n_y}(2j_y+1)e^{-\frac{\lambda}{2}j_y(j_y+1)y}D^{j_y}_{\tilde m_y\tilde n_y}(g_\varphi^{-1})^yD^{j_y}_{\tilde n_y\tilde m_y}(e^{\epsilon_\varphi((A_1\tau_2-A_2\tau_1)\sin\theta)}e^{i\frac{\lambda\delta_\varphi^2}{\kappa\gamma}(E^1\tau_2-E^2\tau_1)})\\ &= \sum_{j_y=0}^{\infty}\sum_{\tilde m_y,\tilde n_y}(2j_y+1)e^{-\frac{\lambda}{2}j_y(j_y+1)}e^{\lambda\tilde m_y\frac{\delta_\varphi^2E^y}{\kappa\gamma}y}D^{j_y}_{\tilde n_y\tilde m_y}(e^{\epsilon_\varphi((A_1\tau_2-A_2\tau_1)\sin\theta)})^yD^{j_y}_{\tilde m_y\tilde n_y}(g_\varphi^{-1}),\end{aligned} \tag{93}$$

where we have used the property

$$\begin{aligned}\chi_{j_\ell}(g_\ell^{-1}G) &= {}^\ell D^{j_\ell}_{\tilde m_\ell\tilde m_\ell}(g_\ell^{-1}G)\\ &= \sum_{n=-j_\ell}^{j_\ell}{}^\ell D^{j_\ell}_{\tilde m_\ell n}(g_\ell^{-1})\,{}^\ell D^{j_\ell}_{n\tilde m_\ell}(G)\\ &= {}^\ell D^{j_\ell}_{\tilde m_\ell\tilde n_\ell}(g_\ell^{-1})\,{}^\ell D^{j_\ell}_{\tilde n_\ell\tilde m_\ell}(G),\end{aligned} \tag{94}$$

and the following relations that we derived in Appendix B,

$$E^x = (E^1\cos\tilde\alpha + E^2\sin\tilde\alpha)\sin\theta = \Lambda R\sin\theta, \tag{95}$$

$$E^y = E^1\cos\tilde\alpha + E^2\sin\tilde\alpha = \Lambda R. \tag{96}$$

Notice that in the coherent state associated with the φ-direction we have not included the $A^3_\varphi = \cos\theta$ component of the connection since this does not enter the reduced phase space (it is conjugate to a flux component that we have gauge fixed) and thus it is not part of the reduced Hilbert space $\mathcal{H}^R$ either. Its contribution to the spherical Euclidean Hamiltonian constraint given in Eq. (34) is encoded in the extra terms that appear in Eq. (24), as already pointed out above.

[11] See also [114] for a previous attempt to investigate singularity resolution through the use of LQG coherent states for a Schwarzschild spacetime.

We can see from Eq. (98) that for $j_x, j_y, j_z \gg 1$ the coefficients $\psi^\lambda_G(j_\ell)$ in the coherent states become Gaussian weights for the fluxes peaked around the semiclassical values $\tilde{j}_\ell = \delta^2_\ell j^0_\ell$, with j^0_ℓ given by

$$j^0_x = \frac{\Lambda R \sin\theta}{\kappa\gamma} = \frac{\sqrt{g_{RR} g_{\varphi\varphi}}}{\kappa\gamma} = \frac{E^\theta_1}{\kappa\gamma\cos\tilde{\alpha}} = \frac{E^\theta_2}{\kappa\gamma\sin\tilde{\alpha}} = \frac{1}{\kappa\gamma}(E^\theta_1\cos\tilde{\alpha} + E^\theta_2\sin\tilde{\alpha}), \tag{97a}$$

$$j^0_y = \frac{\Lambda R}{\kappa\gamma} = \frac{\sqrt{g_{RR} g_{\theta\theta}}}{\kappa\gamma} = -\frac{E^\varphi_1}{\kappa\gamma\sin\tilde{\alpha}} = \frac{E^\varphi_2}{\kappa\gamma\cos\tilde{\alpha}} = \frac{1}{\kappa\gamma}(-E^\varphi_1\sin\tilde{\alpha} + E^\varphi_2\cos\tilde{\alpha}), \tag{97b}$$

$$j^0_z = \frac{R^2\sin\theta}{\kappa\gamma} = \frac{g_{\varphi\varphi}}{\kappa\gamma\sin\theta} = \frac{E^r_3}{\kappa\gamma}, \tag{97c}$$

and $\delta^2_x = \epsilon_r\epsilon_\varphi$, $\delta^2_y = \epsilon_r\epsilon_\theta$, $\delta^2_z = \epsilon_\theta\epsilon_\varphi$.

Let us write the quantum reduced coherent states in the compact notation

$$\psi^\lambda_G(g_\ell) = \sum_{j_\ell=0}^{\infty} \sum_{\bar{m}_\ell,\bar{n}_\ell=\pm j_\ell} (2j_\ell+1)(\psi^\lambda_G)^{j_\ell}_{\bar{n}_\ell\bar{m}_\ell}\, {}^{\ell}D^{j_\ell}_{\bar{m}_\ell\bar{n}_\ell}(g^{-1}_\ell), \tag{98}$$

with the matrix coefficients $(\psi^\lambda_G)^{j_\ell}_{\bar{n}_\ell\bar{m}_\ell}$ explicitly given by Eqs. (91)–(93).

Finally, we can define the normalized quantum reduced coherent states as

$$\widetilde{\psi^\lambda_G}(g_\ell) = \frac{\psi^\lambda_G(g_\ell)}{|\psi^\lambda_G(g_\ell)|}, \tag{99}$$

where

$$|\psi^\lambda_G(g_\ell)| = \sqrt{\sum_{j_\ell=0}^{\infty} \sum_{\bar{m}_\ell,\bar{n}_\ell=\pm j_\ell} |(\psi^\lambda_G)^{j_\ell}_{\bar{n}_\ell\bar{m}_\ell}|^2}. \tag{100}$$

Let us conclude this section by defining the coherent state associated to the reduced spin network state used in Eq. (85) to compute the action of the reduced Euclidean Hamiltonian constraint on it. By including also the faces in the (r,θ)-plane and (r,φ)-plane, the reduced spin network state reads

$|v^R_\square\rangle =$ 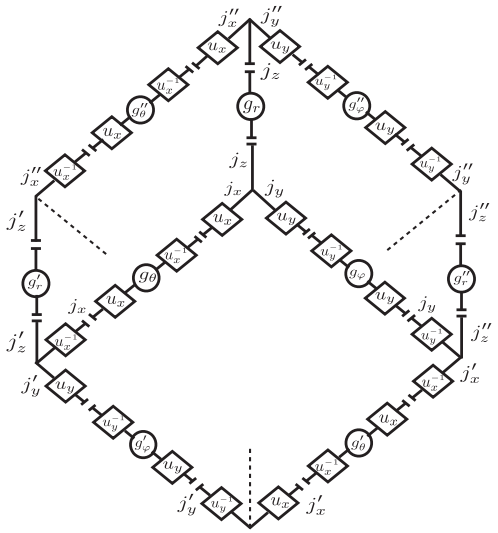 . (101)

The associated normalized quantum reduced coherent state is then given by

$$|\widetilde{\psi^{\lambda}_{\square}}\rangle = \prod_{\ell=x,y,z} \sum_{j_\ell,j'_\ell,j''_\ell=0}^{\infty} \sum_{\bar{m}_\ell,\bar{n}_\ell=\pm j_\ell} \sum_{\bar{m}'_\ell,\bar{n}'_\ell=\pm j'_\ell} \sum_{\bar{m}''_\ell,\bar{n}''_\ell=\pm j''_\ell}$$

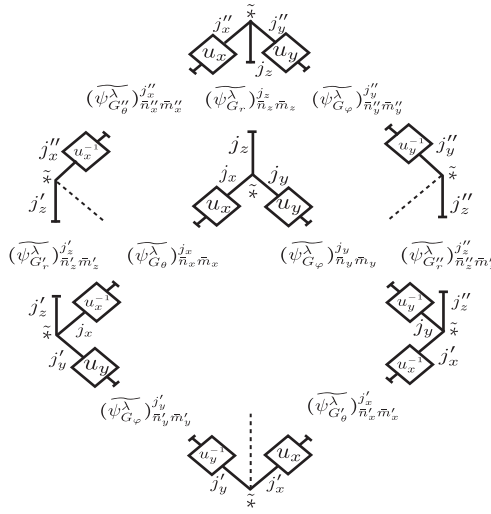

$$|\widetilde{\upsilon^{R}_{\square}}\rangle\,, \tag{102}$$

where for each 3-valent vertex in the state defined in Eq. (101) we have used the norm given in Eq. (76) and we have introduced the notation

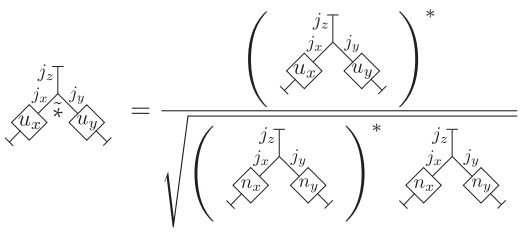

$$= \frac{\left(\quad \right)^{*}}{\sqrt{\left(\quad \right)^{*} \quad}}\,, \tag{103}$$

in order to include the full normalization of the coherent state wave function.

VII. EFFECTIVE HAMILTONIAN

We are now ready to compute the expectation value of the reduced Hamiltonian constraint on the coherent state that we define in Eq. (102) based on a single cuboidal cell of the spatial manifold triangulation by means of the action given in Eq. (85) and its analogue on the other two orthogonal planes.

A. Euclidean term

Let us start with the Euclidean Hamiltonian constraint operator whose action on the basis of $\mathcal{H}^R$ was computed in Eq. (85) for one choice of tangent loop. For the other two possibilities it is straightforward to see that a similar result holds, as already explained at the end of Sec. V A. If we now use this action to compute the expectation value on the normalized coherent state of the form given in Eq. (102), by means of the normalized coherent state wave function properties we obtain the following result:

$$\begin{aligned}
\langle \widetilde{\psi^{\lambda}_{\square}}|{}^{R}\hat{H}^{E}_{\square}[N]|\widetilde{\psi^{\lambda}_{\square}}\rangle \approx -2\sqrt{\frac{\gamma}{\kappa}}N(v) \sum_{\mu=\pm 1/2} s(\mu) \\
\times \Big(\sqrt{\tilde{j}_z\tilde{j}_y(\tilde{j}_x+\mu)}\,\mathrm{Tr}[\tau_x e^{\epsilon_\varphi((A_1(r)\tau_2-A_2(r)\tau_1)\sin\theta)} e^{\epsilon_r A_r(r)\tau_3} e^{-\epsilon_\varphi((A_1(r+\epsilon_r)\tau_2-A_2(r+\epsilon_r)\tau_1)\sin\theta)} e^{-\epsilon_r A_r(r+\epsilon_r)\tau_3}] \\
- \sqrt{\tilde{j}_z\tilde{j}_x(\tilde{j}_y+\mu)}\,\mathrm{Tr}[\tau_y e^{\epsilon_\theta(A_1(r)\tau_1+A_2(r)\tau_2)} e^{\epsilon_r A_r(r)\tau_3} e^{-\epsilon_\theta(A_1(r+\epsilon_r)\tau_1+A_2(r+\epsilon_r)\tau_2)} e^{-\epsilon_r A_r(r+\epsilon_r)\tau_3}] \\
+ \sqrt{\tilde{j}_x\tilde{j}_y(\tilde{j}_z+\mu)}\,\mathrm{Tr}[\tau_3 e^{\epsilon_\theta(A_1(r)\tau_1+A_2(r)\tau_2)} e^{\epsilon_\varphi((A_1(r)\tau_2-A_2(r)\tau_1)\sin(\theta+\epsilon_\theta))} \\
\times e^{-\epsilon_\theta(A_1(r)\tau_1+A_2(r)\tau_2)} e^{-\epsilon_\varphi((A_1(r)\tau_2-A_2(r)\tau_1)\sin\theta)}] \Big)
\end{aligned}$$

$$
\begin{aligned}
&\approx -2\sqrt{\frac{\gamma}{\kappa}}\frac{N(v)}{\sqrt{j_x^0 j_y^0 j_z^0}}\\
&\times (\epsilon_\theta j_z^0 j_y^0 \mathrm{Tr}[\tau_x e^{\epsilon_\varphi((A_1(r)\tau_2-A_2(r)\tau_1)\sin\theta)} e^{\epsilon_r A_r(r)\tau_3} e^{-\epsilon_\varphi((A_1(r+\epsilon_r)\tau_2-A_2(r+\epsilon_r)\tau_1)\sin\theta)} e^{-\epsilon_r A_r(r+\epsilon_r)\tau_3}]\\
&- \epsilon_\varphi j_z^0 j_x^0 \mathrm{Tr}[\tau_y e^{\epsilon_\theta(A_1(r)\tau_1+A_2(r)\tau_2)} e^{\epsilon_r A_r(r)\tau_3} e^{-\epsilon_\theta(A_1(r+\epsilon_r)\tau_1+A_2(r+\epsilon_r)\tau_2)} e^{-\epsilon_r A_r(r+\epsilon_r)\tau_3}]\\
&+ \epsilon_r j_x^0 j_y^0 \mathrm{Tr}[\tau_3 e^{\epsilon_\theta(A_1(r)\tau_1+A_2(r)\tau_2)} e^{\epsilon_\varphi((A_1(r)\tau_2-A_2(r)\tau_1)\sin(\theta+\epsilon_\theta))}\\
&\times e^{-\epsilon_\theta(A_1(r)\tau_1+A_2(r)\tau_2)} e^{-\epsilon_\varphi((A_1(r)\tau_2-A_2(r)\tau_1)\sin\theta)}])\\
&= -\frac{2}{\kappa}\frac{N(v)}{\sqrt{\det(E)}}\\
&\times \left[-\epsilon_\theta E_3^r(-E_1^\varphi\sin\tilde{\alpha}+E_2^\varphi\cos\tilde{\alpha})[ie^{-i\tilde{\alpha}-\frac{i}{2}(A_r(r)+A_r(r+\epsilon_r))\epsilon_r-\frac{1}{2}(\sqrt{-A_1^2(r)-A_2^2(r)}+\sqrt{-A_1^2(r+\epsilon_r)-A_2^2(r+\epsilon_r)})\sin\theta\epsilon_\varphi}\right]\\
&\times \left(\left(1+e^{\sqrt{-A_1^2(r)-A_2^2(r)}\sin\theta\epsilon_\varphi}\right)\left(-1+e^{\sqrt{-A_1^2(r+\epsilon_r)-A_2^2(r+\epsilon_r)}\sin\theta\epsilon_\varphi}\right)\sqrt{-A_1^2(r)-A_2^2(r)}\right.\\
&\times ((e^{2i\tilde{\alpha}}-e^{i(A_r(r)+A_r(r+\epsilon_r))\epsilon_r})A_1(r+\epsilon_r)-i(e^{2i\tilde{\alpha}}+e^{i(A_r(r)+A_r(r+\epsilon_r))\epsilon_r})A_2(r+\epsilon_r))\\
&+\left(-1+e^{\sqrt{-A_1^2(r)-A_2^2(r)}\sin\theta\epsilon_\varphi}\right)\left(1+e^{\sqrt{-A_1^2(r+\epsilon_r)-A_2^2(r+\epsilon_r)}\sin\theta\epsilon_\varphi}\right)\\
&\times\left.\left(-e^{i(2\tilde{\alpha}+A_r(r)\epsilon_r)}(A_1(r)-iA_2(r))+e^{iA_r(r+\epsilon_r)\epsilon_r}(A_1(r)+iA_2(r))\right)\sqrt{-A_1^2(r+\epsilon_r)-A_2^2(r+\epsilon_r)}\right)\\
&/\left(8\sqrt{-A_1^2(r)-A_2^2(r)}\sqrt{-A_1^2(r+\epsilon_r)-A_2^2(r+\epsilon_r)}\right)\\
&+\epsilon_\varphi E_3^r(E_1^\theta\cos\tilde{\alpha}+E_2^\theta\sin\tilde{\alpha})\left[ie^{-i\tilde{\alpha}-\frac{i}{2}(A_r(r)+A_r(r+\epsilon_r))\epsilon_r-\frac{1}{2}(\sqrt{-A_1^2(r)-A_2^2(r)}+\sqrt{-A_1^2(r+\epsilon_r)-A_2^2(r+\epsilon_r)})\epsilon_\theta}\right]\\
&\times\left(\left(1+e^{\sqrt{-A_1^2(r)-A_2^2(r)}\epsilon_\theta}\right)\left(-1+e^{\sqrt{-A_1^2(r+\epsilon_r)-A_2^2(r+\epsilon_r)}\epsilon_\theta}\right)\sqrt{-A_1^2(r)-A_2^2(r)}\right.\\
&\times(-(e^{2i\tilde{\alpha}}-e^{i(A_r(r)+A_r(r+\epsilon_r))\epsilon_r})A_1(r+\epsilon_r)+i(e^{2i\tilde{\alpha}}+e^{i(A_r(r)+A_r(r+\epsilon_r))\epsilon_r})A_2(r+\epsilon_r))\\
&-\left(-1+e^{\sqrt{-A_1^2(r)-A_2^2(r)}\epsilon_\theta}\right)\left(1+e^{\sqrt{-A_1^2(r+\epsilon_r)-A_2^2(r+\epsilon_r)}\epsilon_\theta}\right)\\
&\times\left.\left(-e^{i(2\tilde{\alpha}+A_r(r)\epsilon_r)}(A_1(r)-iA_2(r))+e^{iA_r(r+\epsilon_r)\epsilon_r}(A_1(r)+iA_2(r))\right)\sqrt{-A_1^2(r+\epsilon_r)-A_2^2(r+\epsilon_r)}\right)\\
&/\left(8\sqrt{-A_1^2(r)-A_2^2(r)}\sqrt{-A_1^2(r+\epsilon_r)-A_2^2(r+\epsilon_r)}\right)\\
&+\epsilon_r(E_1^\theta\cos\tilde{\alpha}+E_2^\theta\sin\tilde{\alpha})(-E_1^\varphi\sin\tilde{\alpha}+E_2^\varphi\cos\tilde{\alpha})\frac{1}{8}e^{-\frac{1}{2}\sqrt{-A_1^2(r)-A_2^2(r)}(2\epsilon_\theta+(\sin\theta+\sin(\theta+\epsilon_\theta))\epsilon_\varphi)}\\
&\times\left.\left(-1+e^{2\sqrt{-A_1^2(r)-A_2^2(r)}\epsilon_\theta}\right)\left(-1+e^{\sqrt{-A_1^2(r)-A_2^2(r)}(\sin\theta+\sin(\theta+\epsilon_\theta))\epsilon_\varphi}\right)\right],
\end{aligned}
\tag{104}
$$

where we have used Eq. (97) of the coherent states to peak the fluxes around their semiclassical values.

If we now expand the lengthy expression above to third order in the ϵ's and use Eq. (97), we get

$$
\begin{aligned}
\langle\tilde{\psi}_\square^\lambda|^R\hat{H}_\square^E[N]|\tilde{\psi}_\square^\lambda\rangle \approx \frac{\epsilon_r\epsilon_\theta\epsilon_\varphi}{\kappa}\frac{N(v)}{\sqrt{\det(E)}}&[E_3^r A_r(E_1^\theta A_1+E_2^\theta A_2)+E_3^r(E_1^\theta A_2'-E_2^\theta A_1')\\
&+\sin\theta(E_3^r A_r(E_2^\varphi A_1-E_1^\varphi A_2)+E_3^r(E_2^\varphi A_2'+E_1^\varphi A_1'))\\
&+\sin\theta(E_1^\theta E_2^\varphi-E_2^\theta E_1^\varphi)(A_1^2+A_2^2)]+o(\epsilon^4),
\end{aligned}
\tag{105}
$$

which matches exactly the classical expression given in Eq. (35) in the limit ϵ_r, ϵ_θ, $\epsilon_\varphi \to 0$, once summed over all the vertices.

In order to obtain the full expression of the spherically symmetric Euclidean Hamiltonian constraint given in Eq. (34), we also need to quantize the extra terms in Eq. (24) coming from the phase space extension of the gauge unfixing procedure. The quantization of all these extra terms would result in a rather complicated operator. However, we know from the classical analysis that only the last term in Eq. (36) will remain. Therefore, in order to simplify the construction of the full Euclidean Hamiltonian constraint, let us just quantize the term

$$ {}^{R}H^{\mathrm{ext}}[N] = \frac{1}{\kappa}\int_{\Sigma} d^3x \frac{N}{\sqrt{\det(E)}} E^A_I \partial_A \partial_B E^{IB}. \tag{106} $$

Following the quantization prescription given in Eq. (87) for the second derivatives of the fluxes, the quantized Euclidean Hamiltonian constraint regularized on a cubic cell dual to a 6-valent node v with coordinates $\{r,\theta,\varphi\}$ and its neighbouring ones is given by

$$ \begin{aligned} {}^{R}\hat{H}^{\mathrm{ext}}_{\square}[N] = {} & \frac{1}{\kappa}\frac{N(v)}{{}^{R}\hat{V}(v)}[{}^{R}\hat{E}_I(S^\theta(r,\theta,\varphi))({}^{R}\hat{E}_I(S^\theta(r,\theta+2\epsilon^\theta,\varphi)) - 2{}^{R}\hat{E}_I(S^\theta(r,\theta+\epsilon^\theta,\varphi)) + {}^{R}\hat{E}_I(S^\theta(r,\theta,\varphi))) \\ & + {}^{R}\hat{E}_I(S^\varphi(r,\theta,\varphi))({}^{R}\hat{E}_I(S^\theta(r,\theta+\epsilon^\theta,\varphi+\epsilon^\varphi)) - {}^{R}\hat{E}_I(S^\theta(r,\theta+\epsilon^\theta,\varphi)) - {}^{R}\hat{E}_I(S^\theta(r,\theta,\varphi+\epsilon^\varphi)) + {}^{R}\hat{E}_I(S^\theta(r,\theta,\varphi))) \\ & + {}^{R}\hat{E}_I(S^\theta(r,\theta,\varphi))({}^{R}\hat{E}_I(S^\varphi(r,\theta+\epsilon^\theta,\varphi+\epsilon^\varphi)) - {}^{R}\hat{E}_I(S^\varphi(r,\theta,\varphi+\epsilon^\varphi)) - {}^{R}\hat{E}_I(S^\varphi(r,\theta+\epsilon^\theta,\varphi)) + {}^{R}\hat{E}_I(S^\varphi(r,\theta,\varphi))) \\ & + {}^{R}\hat{E}_I(S^\varphi(r,\theta,\varphi))({}^{R}\hat{E}_I(S^\varphi(r,\theta,\varphi+2\epsilon^\varphi)) - 2{}^{R}\hat{E}_I(S^\varphi(r,\theta,\varphi+\epsilon^\varphi)) + {}^{R}\hat{E}_I(S^\varphi(r,\theta,\varphi)))]. \end{aligned} \tag{107} $$

When computing its expectation value on the coherent state defined in Eq. (102), it is immediate to see that only the first line on the right-hand side of the expression above contributes. Therefore we get

$$ \begin{aligned} \langle\tilde{\psi^\lambda_\square}|{}^{R}\hat{H}^{\mathrm{ext}}_{\square}[N]|\tilde{\psi^\lambda_\square}\rangle &\approx \frac{1}{\kappa}\frac{\epsilon_r\epsilon_\varphi}{\epsilon_\theta}\frac{N(v)}{\sqrt{\det(E)}}(E^\theta_1E^\varphi_2 - E^\theta_2E^\varphi_1)[\sin(\theta+2\epsilon_\theta) - 2\sin(\theta+\epsilon_\theta) + \sin\theta] \\ &\approx -\frac{\epsilon_r\epsilon_\theta\epsilon_\varphi}{\kappa}\frac{N(v)}{\sqrt{\det(E)}}(E^\theta_1E^\varphi_2 - E^\theta_2E^\varphi_1)\sin\theta + o(\epsilon^4). \end{aligned} \tag{108} $$

Therefore, at the leading order we recover

$$ \sum_{\square}\langle\tilde{\psi^\lambda_\square}|({}^{R}\hat{H}^{E}_{\square}[N] + {}^{R}\hat{H}^{\mathrm{ext}}_{\square}[N])|\tilde{\psi^\lambda_\square}\rangle \approx H^E_{\mathrm{sph}}[N] + o(\epsilon^4), \tag{109} $$

showing how our construction exhibits the correct semiclassical limit.

We can now write the first order correction to the classical expression of the reduced Euclidean Hamiltonian constraint above. This is obtained by looking at the terms of order four in ϵ in Eq. (104) as well as in Eq. (107). We find

$$ \begin{aligned} \langle\tilde{\psi^\lambda_\square}|{}^{R}\hat{H}^{E}_{\square}[N] + {}^{R}\hat{H}^{\mathrm{ext}}_{\square}[N]|\tilde{\psi^\lambda_\square}\rangle_{(1)} \approx {} & \frac{\epsilon_r\epsilon_\theta\epsilon_\varphi}{\kappa}\frac{N(v)}{\sqrt{\det(E)}}\Big[\frac{1}{2}E^r_3(E^\theta_1(-A_r^2A_2 + 2A_rA_1' + A_2'') + E^\theta_2(A_r^2A_1 + 2A_rA_2' - A_1''))\epsilon_r \\ & - \frac{\sin\theta}{2}E^r_3(E^\varphi_2(A_r^2A_2 - 2A_rA_1' - A_2'') + E^\varphi_1(A_r^2A_1 + 2A_rA_2' - A_1''))\epsilon_r \\ & - \frac{\sin(2\theta)}{4}(E^r_3A_r(E^\varphi_2A_2 + E^\varphi_1A_1) + E^r_3(E^\varphi_1A_2' - E^\varphi_2A_1'))\epsilon_\varphi \\ & + \cos\theta(E^\theta_1E^\varphi_2 - E^\theta_2E^\varphi_1)(A_1^2 + A_2^2 - 1)\epsilon_\theta\Big] \\ = {} & \frac{\epsilon_r\epsilon_\theta\epsilon_\varphi}{\kappa}\frac{N(v)}{\sqrt{((E^1)^2 + (E^2)^2)E^r}} \\ & \times\Big[\sin\theta E^r(E^1(-A_r^2A_2 + 2A_rA_1' + A_2'') + E^2(A_r^2A_1 + 2A_rA_2' - A_1''))\epsilon_r \\ & + \cos\theta((E^1)^2 + (E^2)^2)(A_1^2 + A_2^2 - 1)\epsilon_\theta \\ & - \frac{\sin(2\theta)}{4}(E^rA_r(E^1A_2 - E^2A_1) - E^r(E^2A_2' + E^1A_1'))\epsilon_\varphi\Big], \end{aligned} \tag{110} $$

where in the last equality we have used Eq. (12). Notice that since the second and the last correction terms proportional to ϵ_θ and ϵ_φ contain an overall θ-dependent part of the form, respectively $\cos\theta$ and $\sin(2\theta)$, in the continuum limit when integrating over $\theta\in[0,\pi]$ they both vanish. However, the first correction term proportional to ϵ_r has an overall θ dependence that survives the integral and it represents the only correction at first order.

Therefore, after performing the sum over all cuboidal cells of the triangulation and taking the continuum limit ϵ_r, ϵ_θ, $\epsilon_\varphi \to 0$, we obtain the effective Euclidean Hamiltonian constraint for a spherically symmetric spacetime given by the quantum corrected expression

$$
\begin{aligned}
{}^{R}H^{E}_{\mathrm{eff}}[N] = \frac{1}{2G}\int_\Sigma dr \frac{N(r)}{\sqrt{((E^1)^2+(E^2)^2)E^r}}[&(2E^r A_r(E^1A_1+E^2A_2)+2E^r(E^1A_2'-E^2A_1')\\
&+((E^1)^2+(E^2)^2)(A_1^2+A_2^2))\\
&+\epsilon_r(E^rA_r(A_rE^2A_1-A_rE^1A_2+2E^1A_1'+2E^2A_2')+E^r(E^1A_2''-E^2A_1'')))].
\end{aligned}
\tag{111}
$$

B. Lorentzian term

The expectation value of the Lorentzian Hamiltonian constraint operator can be computed using its expression in terms of the densitized scalar curvature expressed as a function of the fluxes and their derivatives alone, as obtained in Eq. (A17). Let us set $\epsilon_\theta = \epsilon_\varphi = \epsilon$ and quantize derivatives of the fluxes again in terms of discrete differences as defined in Eqs. (86) and (87). We have

$$
\begin{aligned}
\langle\tilde{\psi^\lambda_\square}|{}^{R}\hat{H}^{L}_{\square}[N]|\tilde{\psi^\lambda_\square}\rangle \approx &\frac{1}{\kappa}\left(1+\frac{1}{\gamma^2}\right)\frac{1}{\epsilon_r^3\epsilon^8}\frac{N(v)}{2(E_3^r)^{5/2}\sqrt{\sin\theta}[(E_1^\varphi)^2+(E_2^\varphi)^2]^{3/2}}\\
&\times[-2(\sin\theta)^2\epsilon^8\epsilon_r^4(E_1^\varphi)^4(E^r)^2[(\sin(\theta+\epsilon)-\sin\theta)^2-\sin\theta(\sin(\theta+2\epsilon)-2\sin(\theta+\epsilon)+\sin\theta)]\\
&-2(\sin\theta)^2\epsilon^8\epsilon_r^4(E_1^\varphi)^3E^2(E^r)^2[(\sin(\theta+\epsilon)-\sin\theta)^2+\sin\theta(\sin(\theta+2\epsilon)-2\sin(\theta+\epsilon)+\sin\theta)]\\
&-2(\sin\theta)^2\epsilon^8\epsilon_r^2E_1^\varphi(E^r)^2(\epsilon_r^2E^2E_2^\varphi[(E_2^\varphi-4E^1)(\sin(\theta+\epsilon)-\sin\theta)^2\\
&+E_2^\varphi\sin\theta(\sin(\theta+2\epsilon)-2\sin(\theta+\epsilon)+\sin\theta)]\\
&-2\epsilon^2(\sin\theta)^2E^r(E^2(r+\epsilon_r)-E^2(r))(E^r(r+\epsilon_r)-E^r(r)))\\
&+(E_1^\varphi)^2(\sin\theta)^2\epsilon^8\epsilon_r^2(E^r)^2(-4\epsilon_r^2(E_2^\varphi)^2[(\sin(\theta+\epsilon)-\sin\theta)^2-\sin\theta(\sin(\theta+2\epsilon)-2\sin(\theta+\epsilon)+\sin\theta)]\\
&+2\epsilon_r^2E_2^\varphi E^1[(\sin(\theta+\epsilon)-\sin\theta)^2+\sin\theta(\sin(\theta+2\epsilon)-2\sin(\theta+\epsilon)+\sin\theta)]\\
&+[4\epsilon_r^2(E^1)^2(\sin(\theta+\epsilon)-\sin\theta)^2+(\sin\theta)^2\epsilon^2(E^r(r+\epsilon_r)-E^r(r))^2\\
&+4(\sin\theta)^2\epsilon^2E^r(r)(E^r(r+2\epsilon_r)-2E^r(r+\epsilon_r)+E^r(r))])\\
&+\epsilon^8\epsilon_r^2E_2^\varphi(\sin\theta)^2(E^r)^2(-2(E_2^\varphi)^3\epsilon_r^2[(\sin(\theta+\epsilon)-\sin\theta)^2-\sin\theta(\sin(\theta+2\epsilon)-2\sin(\theta+\epsilon)+\sin\theta)]\\
&+2(E_2^\varphi)^2\epsilon_r^2E^1[(\sin(\theta+\epsilon)-\sin\theta)^2+\sin\theta(\sin(\theta+2\epsilon)-2\sin(\theta+\epsilon)+\sin\theta)]\\
&-4\epsilon^2(\sin\theta)^2E^r(E^1(r+\epsilon_r)-E^1(r))(E^r(r+\epsilon_r)-E^r(r))\\
&+E_2^\varphi[4\epsilon_r^2(E^2)^2(\sin(\theta+\epsilon)-\sin\theta)^2+\epsilon^2(\sin\theta)^2[(E^r(r+\epsilon_r)-E^r(r))^2\\
&+4E^r(E^r(r+2\epsilon_r)-2E^r(r+\epsilon_r)+E^r(r))]])]\\
=&\frac{1}{\kappa}\left(1+\frac{1}{\gamma^2}\right)\frac{N(v)}{2\sqrt{E^r}[(E^1(r))^2+(E^2(r))^2]^{3/2}}\\
&\times[4\epsilon_r[(E^2(r))^2+(E^1(r))^2]^2(\sin(\theta+2\epsilon)-2\sin(\theta+\epsilon)+\sin\theta)\\
&+\frac{\epsilon^2}{\epsilon_r}\sin\theta[(E^1(r))^2+(E^2(r))^2]((E^r(r+\epsilon_r)-E^r(r))^2+4E^r(r)(E^r(r+2\epsilon_r)-2E^r(r+\epsilon_r)+E^r(r)))\\
&-4\frac{\epsilon^2}{\epsilon_r}\sin\theta E^r(r)(E^r(r+\epsilon_r)-E^r(r))[E^1(r)(E^1(r+\epsilon_r)-E^1(r))+E^2(r)(E^2(r+\epsilon_r)-E^2(r))]].
\end{aligned}
\tag{112}
$$

By expanding the above expression for the expectation value up to the fourth order in ϵ's, we get

$$\begin{aligned}\langle\tilde{\psi^{\lambda}_{\square}}|{}^{R}\hat{H}^{L}_{\square}[N]|\tilde{\psi^{\lambda}_{\square}}\rangle \approx{}& \frac{1}{\kappa}\left(1+\frac{1}{\gamma^2}\right)\frac{\epsilon_r\epsilon^2 N(v)}{2\sqrt{E^r}[(E^1(r))^2+(E^2(r))^2]^{3/2}}\\ &\times[-4\sin\theta[(E^2(r))^2+(E^1(r))^2]^2\\ &+\sin\theta[(E^1(r))^2+(E^2(r))^2]((E^{r'}(r))^2+4E^r(r)E^{r''}(r))\\ &-4\sin\theta E^r(r)E^{r'}(r)[E^1(r)E^{1'}(r)+E^2(r)E^{2'}(r)]\\ &-4\epsilon\cos\theta[(E^2(r))^2+(E^1(r))^2]^2\\ &+\epsilon_r\sin\theta[[(E^1(r))^2+(E^2(r))^2](E^{r'}(r)E^{r''}(r)+4E^r(r)E^{r'''}(r))\\ &-2E^r(r)[E^1(r)(E^{r'}E^{1''}(r)+E^{r''}E^{1'}(r))+E^2(r)(E^{r'}E^{2''}(r)+E^{r''}E^{2'}(r))]]] \end{aligned} \tag{113}$$

$$\begin{aligned}={}& \frac{2}{\kappa}\left(1+\frac{1}{\gamma^2}\right)\epsilon_r\epsilon^2 N(v)\\ &\times\left\{\sin\theta\left[\Lambda(r)\left(\frac{(R'(r))^2}{\Lambda^2(r)}-1\right)+2\frac{R(r)}{\Lambda(r)}\left(R''(r)-\frac{\Lambda'(r)R'(r)}{\Lambda(r)}\right)\right]\right.\\ &+\epsilon_r\frac{\sin\theta}{\Lambda(r)}\left[2R'(r)R''(r)+2R(r)R'''(r)-3\frac{\Lambda'(r)(R'(r))^2}{\Lambda(r)}-\frac{\Lambda''(r)R(r)R'(r)}{\Lambda(r)}-2\frac{\Lambda'(r)R(r)R''(r)}{\Lambda(r)}\right]\\ &\left.-\epsilon\cos\theta\Lambda(r)\right\}. \end{aligned} \tag{114}$$

We see that the leading term in the last equality above reproduces the classical expression given in Eq. (40) for the Lorentzian part of the Hamiltonian constraint. The last two subleading terms correspond to quantum corrections. However, notice that the second correction term proportional to ϵ vanishes when the integral over θ is performed and only the correction proportional to ϵ_r remains. Equivalently, the classical and the correction terms' expressions in terms of densitized triads can be read off of the first equality in Eq. (113).

VIII. CONCLUDING REMARKS

In this article we laid the foundations for a systematic treatment of spherically symmetric spacetimes in the framework of LQG. Applying the QRLG proposal, we implemented a quantization program that is aimed at identifying a symmetric sector at the quantum level, thus reverting the process of symmetry reduction and quantization that is frequently adopted in all existing treatments of quantum black holes. The main result of this paper is the construction of an effective Hamiltonian that can now be used to evolve black hole initial data sets while incorporating quantum corrections. To construct this Hamiltonian, we first built a convenient quantum gauge fixed kinematical Hilbert space that is compatible with a radial gauge even in the absence of symmetry. This was used to define coherent states where a notion of spherical symmetry could be imposed at the level of expectation values of geometrical operators. We then quantized the modified Hamiltonian constraint resulting from the gauge unfixing procedure as explained in Sec. III. Finally we computed the effective Hamiltonian as the expectation value of the modified Hamiltonian operator on the coherent states that, if sharply peaked, are the best candidates to describe classical geometries.

The classical data entering the coherent states can now be seen as the initial data set to be evolved with the effective Hamiltonian. The importance of our result lies in the fact that it is not tied to a particular choice of foliation, allowing one to treat on equal footing various sets of coordinate systems such as horizon penetrating coordinates or coordinates restricted to the interior or exterior of the event horizon of a black hole. This is a significant addition to the existing literature that mainly deals with either the interior or the exterior of event horizons. In most of the previous treatments of this problem, one has been forced to use different Hilbert spaces for the interior and the exterior (as a result of the classical symmetry reduction process) which is normally plagued by ambiguities associated with gluing together interior and exterior geometries.[12]

[12]In the symmetry reduced phase space quantization scheme of [62,63,115] one is still able to use the same kinematical Hilbert space for the solutions to the Hamiltonian constraint both in the exterior and the interior, in the sense that they have a finite norm with respect to the same inner product. However, one of the quantum numbers characterizing the solutions changes from real to pure imaginary when going from the exterior to the interior. This implies that, effectively, one ends up treating the two regions separately and the structure of the complete solution at the horizon is not specified, leaving the gluing ambiguity. Let us also point out that the Hamiltonian that is quantized in [62,115] corresponds to the correct equation of motion on shell but it results in an algebra that is not equivalent to Dirac algebra restricted to the symmetric subspace. Here, in contrast, we deal with the original set of constraints.

We are now in a position to study the equation of motion generated by the effective Hamiltonian. In the forthcoming works we will present the dressed metric that incorporates the quantum corrections and verify its compatibility with the existing results based on polymerlike quantization that is used in LQC or the proposed Planck star metric. In particular, it was shown in the cosmological context that scenarios different from a symmetric or asymmetric bounce are possible[13] and it would be interesting to explore the consequences of this type of singularity resolution on the black hole–white hole scenario. Our final aim in the foreseeable future is to solve the quantum gravitational collapse problem in the presence of matter through the simplifications introduced by the QRLG approach, which facilitates the inclusion of extra fields [116,117].

Another important application of our construction that is related to the issues of singularity resolution and the black hole information loss paradox is to illuminate the quantum nature of black hole entropy. This problem has quite a long history in the LQG literature. The first ideas on how to microscopically describe the d.o.f. accounting for the Bekenstein-Hawking entropy formula date back to the works [118–120]. This approach was then refined within the framework of "isolated horizons" in [121–123] and generalized to the full gauge-invariant case in [124–128]. Despite the remarkable success of these results in recovering the entropy-area law from a quantum description of the horizon gravitational d.o.f., there are two open issues that still affect the LQG derivation of black hole entropy. The first concerns the role of the Barbero-Immirzi parameter in recovering the exact numerical coefficient $1/4$ in the Bekenstein-Hawking entropy formula (see [129–138] for an extensive debate on this topic). The second somehow unsatisfactory feature of the LQG black hole entropy calculation that is oftentimes simply glossed over is the *assumption* of the validity of the "weak holographic principle," [139] leading to a horizon density matrix in which *both* the interior and the exterior of the black hole quantum geometry d.o.f. are traced over.

Our construction has the potential to solve both issues, or at least to provide important insights about them. In fact, concerning the fixation of the Barbero-Immirzi parameter, it has recently been pointed out in the literature [76,77,132,140,141] that new d.o.f. should be included in the partition function in order to set γ free from any numerical constraint.[14] This is in addition to the internal gauge d.o.f. already accounted for in the standard calculation. These new d.o.f. have been identified with either graph combinatorial structures or inclusion of matter (see, however, [140] for a possible unification of the two). Since our construction of a spherically symmetric black hole quantum geometry derives from the full theory and does not rely on Chern-Simons techniques to model the horizon as a single intertwiner Hilbert space, new horizon graph d.o.f. are automatically included in the horizon partition function. At the same time, inclusion of matter can be implemented in a straightforward manner as pointed out above. This provides the possibility to investigate the role of the Barbero-Immirzi parameter in the entropy calculation through a physically richer modelization of the horizon quantum geometry.

Concerning the validity of the weak holographic principle, i.e., the idea that the d.o.f. relevant to the Bekenstein-Hawking entropy formula are only those lying at the horizon and in its vicinity, this is expected to be proven by the implementation of the quantum dynamics. More precisely, it is the solution of the Hamiltonian constraint, as well as the implementation of semiclassical consistency conditions, that should introduce correlations between the horizon and the interior d.o.f. In fact, contrary to the AdS/CFT proposal, we expect the notion of holography to emerge only at the semiclassical level (see, e.g., [25] for a discussion of this point of view). An intriguing scenario would be the possibility to construct physical solutions from the repeated action of the Hamiltonian constraint operator on a seed state, along the lines of the GFT condensates philosophy [76,77] but now with a concrete notion of the dynamics at hand. This could allow for the construction of a physical black hole interior density matrix given by a weighted sum over graphs with weights provided by matrix elements of the Hamiltonian constraint. In this picture then, a concrete notion of holography could be described and tested by understanding how dynamics is implemented as a refinement operation and by going to a continuum limit by means of coarse graining techniques, in the spirit of [143,144]. This is clearly a very ambitious and long-term plan that we leave for future investigations. However, all the necessary ingredients and tools are now at our disposal.

ACKNOWLEDGMENTS

We acknowledge the John Templeton Foundation for the supporting Grant No. 51876. This work was supported in part by the National Science Foundation (NSF) Grant No. PHY-1505411, the Eberly research funds of Penn State, and the grant of Polish Narodowe Centrum Nauki No. DEC-2011/02/A/ST2/00300. Research at the Perimeter Institute for Theoretical Physics is supported in part by the Government of Canada through Natural Sciences and Engineering Research Council (NSERC) and by the Province of Ontario through Ministry of Research and Innovation (MRI).

[13]Namely, the emergent bouncing Universe [90].

[14]A possible source of the ambiguity behind the role of γ may also be related to the issue pointed out in [142], namely the inadequacy of the isolated horizon boundary condition usually implemented in the quantum theory to single out the notion of a horizon. The characterization of an isolated horizon through new d.o.f. emerging from some particular boundary conditions, as well as through a maximal entropy principle, may settle this ambiguity.

APPENDIX A: CONNECTION COEFFICIENTS AND CURVATURE FOR GEOMETRIES IN SPHERICAL SYMMETRY

The components of an antisymmetric spin connection solution to the torsion-free equation $de^I = -\omega^I{}_J \wedge e^J$ can be written as

$$\omega_{IJ} = \frac{1}{2}(c_{IJK} + c_{IKJ} - c_{JKI})e^K, \tag{A1}$$

where c_{IJK} are the structure functions. Using this one can read off the expression

$$de^I = -\frac{1}{2}c_{JK}{}^I e^J \wedge e^K. \tag{A2}$$

From Eq. (8a) we have

$$\begin{aligned}
de^0 &= N' dr \wedge dt = \frac{N'}{N\Lambda} e^3 \wedge e^0, \\
de^3 &= (\Lambda' N^r + \Lambda N^{r\prime})dr \wedge dt - \dot{\Lambda} dr \wedge dt = \frac{(\Lambda' N^r + \Lambda N^{r\prime} - \dot{\Lambda})}{N\Lambda} e^3 \wedge e^0, \\
de^1 &= R' \cos\alpha dr \wedge d\theta - R' \sin\theta \sin\alpha dr \wedge d\varphi \\
&\quad + \dot{R} \cos\alpha dt \wedge d\theta - \dot{R} \sin\theta \sin\alpha dt \wedge d\varphi \\
&\quad - R \cos\theta \sin\alpha d\theta \wedge d\varphi \\
&= \frac{R'}{R\Lambda} e^3 \wedge e^1 + \frac{(\dot{R} - R' N^r)}{RN} e^0 \wedge e^1 - \frac{\cot\theta \sin\alpha}{R} e^1 \wedge e^2, \\
de^2 &= R' \sin\alpha dr \wedge d\theta + R' \sin\theta \cos\alpha dr \wedge d\varphi \\
&\quad + \dot{R} \sin\alpha dt \wedge d\theta + \dot{R} \sin\theta \cos\alpha dt \wedge d\varphi \\
&\quad + R \cos\theta \cos\alpha d\theta \wedge d\varphi \\
&= \frac{R'}{R\Lambda} e^3 \wedge e^2 + \frac{(\dot{R} - R' N^r)}{RN} e^0 \wedge e^2 + \frac{\cot\theta \cos\alpha}{R} e^1 \wedge e^2.
\end{aligned}$$

Using Eq. (A2), the corresponding nonvanishing structure functions are

$$\begin{aligned}
c_{30}{}^0 &= -c_{03}{}^0 = -\frac{N'}{N\Lambda} \\
c_{30}{}^3 &= -c_{03}{}^3 = -\frac{(\Lambda' N^r + \Lambda N^{r\prime} - \dot{\Lambda})}{N\Lambda} \\
c_{01}{}^1 &= -c_{10}{}^1 = \frac{R' N^r - \dot{R}}{R\Lambda} \\
c_{02}{}^2 &= -c_{20}{}^2 = \frac{R' N^r - \dot{R}}{R\Lambda} \\
c_{31}{}^1 &= -c_{13}{}^1 = -\frac{R'}{R\Lambda} \\
c_{12}{}^1 &= -c_{21}{}^1 = \frac{\cot\theta \sin\alpha}{R} \\
c_{32}{}^2 &= -c_{23}{}^2 = -\frac{R'}{R\Lambda} \\
c_{12}{}^2 &= -c_{21}{}^2 = -\frac{\cot\theta \cos\alpha}{R}.
\end{aligned}$$

We insert these in Eq. (A1) and find

$$\omega_{03} = -\frac{N'}{N\Lambda}e^0 + \frac{(\Lambda' N^r + \Lambda N^{r\prime} - \dot{\Lambda})}{N\Lambda}e^3 = \left(\frac{N^r}{N}(\Lambda' N^r + \Lambda N^{r\prime} - \dot{\Lambda}) - \frac{N'}{\Lambda}\right)dt + \frac{(\Lambda' N^r + \Lambda N^{r\prime} - \dot{\Lambda})}{N}dr, \tag{A3a}$$

$$\omega^{01} = -\omega_{01} = \frac{(R' N^r - \dot{R})}{R\Lambda}e^1 = \frac{(R' N^r - \dot{R})}{\Lambda}\cos\alpha d\theta - \frac{(R' N^r - \dot{R})}{\Lambda}\sin\theta\sin\alpha d\varphi, \tag{A3b}$$

$$\omega^{02} = -\omega_{02} = \frac{(R' N^r - \dot{R})}{R\Lambda}e^2 = \frac{(R' N^r - \dot{R})}{\Lambda}\sin\alpha d\theta + \frac{(R' N^r - \dot{R})}{\Lambda}\sin\theta\cos\alpha d\varphi, \tag{A3c}$$

$$\omega^{12} = \frac{\cot\theta\sin\alpha}{R}e^1 - \frac{\cot\theta\cos\alpha}{R}e^2 = -\cos\theta d\varphi, \tag{A3d}$$

$$\omega^{13} = \frac{R'}{R\Lambda}e^1 = \frac{R'}{\Lambda}(\cos\alpha d\theta - \sin\theta\sin\alpha d\varphi), \tag{A3e}$$

$$\omega^{23} = \frac{R'}{R\Lambda}e^2 = \frac{R'}{\Lambda}(\sin\alpha d\theta + \sin\theta\cos\alpha d\varphi). \tag{A3f}$$

For the connection coefficients $\Gamma^i_a = -\frac{1}{2}\epsilon^i{}_{jk}\omega^{jk}_a$, from the expressions above we obtain

$$\Gamma^1_\varphi = -\sin\theta\Gamma^2_\theta = -\cos\alpha\sin\theta\frac{R'}{\Lambda}, \tag{A4a}$$

$$\Gamma^2_\varphi = \sin\theta\Gamma^1_\theta = -\sin\alpha\sin\theta\frac{R'}{\Lambda}, \tag{A4b}$$

$$\Gamma^3_\varphi = \cos\theta, \tag{A4c}$$

$$\Gamma^i_r = 0, \tag{A4d}$$

from which we compute the intrinsic curvature components $R^k_{ab} = 2\partial_{[a}\Gamma^k_{b]} + \epsilon^k{}_{lm}\Gamma^l_a\Gamma^m_b$,

$$R^1_{r\varphi} = -\sin\theta R^2_{r\theta} = \partial_r\Gamma^1_\varphi = -\cos\alpha\sin\theta\left(\frac{R''}{\Lambda} - \frac{R'\Lambda'}{\Lambda^2}\right), \tag{A5a}$$

$$R^2_{r\varphi} = \sin\theta R^1_{r\theta} = \partial_r\Gamma^2_\varphi = -\sin\alpha\sin\theta\left(\frac{R''}{\Lambda} - \frac{R'\Lambda'}{\Lambda^2}\right), \tag{A5b}$$

$$R^3_{\theta\varphi} = \partial_\theta\Gamma^3_\varphi + 2\Gamma^{[1}_\theta\Gamma^{2]}_\varphi = \sin\theta\left(\frac{(R')^2}{\Lambda^2} - 1\right) \tag{A5c}$$

$$R^1_{\theta\varphi} = R^2_{\theta\varphi} = 0, \tag{A5d}$$

and

$$R = -\epsilon_{ijk}R^k_{ab}e^a_i e^b_j = 4e^r_3(R^1_{r\theta}e^\theta_2 - R^2_{r\theta}e^\theta_1) + 2R^3_{\theta\varphi}(e^\theta_2 e^\varphi_1 - e^\theta_1 e^\varphi_2) = \frac{4}{R\Lambda^2}\left(\frac{R'\Lambda'}{\Lambda} - R''\right) + \frac{2}{R^2}\left(1 - \frac{(R')^2}{\Lambda^2}\right). \tag{A6}$$

For the components of the Ashtekar-Barbero connection $A^i_a = \Gamma^i_a + \gamma K^i_a$, namely $F^i_{ab}(A) = 2\partial_{[a}A^i_{b]} + \epsilon^i{}_{jk}A^j_a A^k_b$, we use Eq. (13) to get

$$F^1_{r\theta}(A) = \partial_r A^1_\theta - A^2_\theta A^3_r = A_1' - A_2 A_r, \tag{A7a}$$

$$F^1_{r\varphi}(A) = \partial_r A^1_\varphi - A^2_\varphi A^3_r = -\sin\theta(A_2' + A_1 A_r), \tag{A7b}$$

$$F^1_{\theta\varphi}(A) = \partial_\theta A^1_\varphi + A^2_\theta A^3_\varphi = 0, \tag{A7c}$$

$$F^2_{r\theta}(A) = \partial_r A^2_\theta + A^1_\theta A^3_r = A_2' + A_1 A_r, \tag{A7d}$$

$$F^2_{r\varphi}(A) = \partial_r A^2_\varphi + A^1_\varphi A^3_r = \sin\theta(A_1' - A_2 A_r), \tag{A7e}$$

$$F^2_{\theta\varphi}(A) = \partial_\theta A^2_\varphi - A^1_\theta A^3_\varphi = 0, \tag{A7f}$$

$$F^3_{r\theta}(A) = F^3_{r\varphi}(A) = 0, \tag{A7g}$$

$$F^3_{\theta\varphi}(A) = \partial_\theta A^3_\varphi + A^1_\theta A^2_\varphi - A^1_\varphi A^2_\theta = \sin\theta[A^2_1 + A^2_2 - 1]. \tag{A7h}$$

1. Densitized scalar curvature in terms of fluxes

Here we express the densitized scalar curvature, $\sqrt{\det(\mathrm{E})}R$, in terms of the fluxes and their derivatives. The final result of this calculation appears in Eq. (40).

The starting equation is

$$\begin{aligned}\sqrt{\det(\mathrm{E})}R &= -\sqrt{\det(E)}\epsilon_{ijk}R^{k}_{ab}e^{a}_{i}e^{b}_{j}\\ &= -\frac{\epsilon_{ijk}}{\sqrt{\det(E)}}E^{a}_{i}E^{b}_{j}(2\partial_{[a}\Gamma^{k}_{b]}+\epsilon^{k}{}_{lm}\Gamma^{l}_{a}\Gamma^{m}_{b}).\end{aligned} \tag{A8}$$

Note that by our gauge condition, the only nonvanishing fluxes are

$$E^{r}_{3}, E^{\theta}_{a}, E^{\theta}_{2}, E^{\varphi}_{1}, E^{\varphi}_{2}. \tag{A9}$$

We are also going to exploit some simplifications resulting from spherical symmetry. Let us emphasize that this is not going to undermine the generality of our quantum result when computing the expectation value of the Lorentzian Hamiltonian constraint operator. This is due to the fact that the coherent states constructed to implement the spherical symmetry enforce these simplifications in the final result for the expectation value. This is just a matter of convenience to avoid even lengthier expressions which in the end yield the same effective result. However, we are not going to use the explicit spherically symmetric expressions for the fluxes within terms containing nonvanishing derivatives (in the spherically symmetric case) since this would yield simplifications which *a priori*, while preserving the semiclassical expression, could remove sources of quantum corrections at higher orders.

So first, as it was also previously shown due to spherical symmetry, the only nonzero Γ^{i}_{a}'s are

$$\Gamma^{1}_{\varphi}, \Gamma^{2}_{\varphi}, \Gamma^{3}_{\varphi}, \Gamma^{1}_{\theta}, \Gamma^{2}_{\theta}. \tag{A10}$$

Additionally, due to spherical symmetry neither the fluxes nor the spin connections depend on the coordinate φ. Taking advantage of these simplifications, Eq. (A8) becomes

$$\begin{aligned}\sqrt{\det(\mathrm{E})}R &= -\frac{\epsilon_{ijk}}{\sqrt{\det(E)}}E^{a}_{i}E^{b}_{j}(2\partial_{[a}\Gamma^{k}_{b]}+\epsilon^{k}{}_{lm}\Gamma^{l}_{a}\Gamma^{m}_{b})\\ &= -\frac{2}{\sqrt{\det(E)}}[E^{a}_{1}E^{b}_{2}(2\partial_{[a}\Gamma^{3}_{b]}+\epsilon^{3}{}_{lm}\Gamma^{l}_{a}\Gamma^{m}_{b})+E^{a}_{2}E^{b}_{3}(2\partial_{[a}\Gamma^{1}_{b]}+\epsilon^{1}{}_{lm}\Gamma^{l}_{a}\Gamma^{m}_{b})+E^{a}_{3}E^{b}_{1}(2\partial_{[a}\Gamma^{2}_{b]}+\epsilon^{2}{}_{lm}\Gamma^{l}_{a}\Gamma^{m}_{b})]\\ &= -\frac{2}{\sqrt{\det(E)}}[E^{a}_{1}E^{b}_{2}(2\partial_{[a}\Gamma^{3}_{b]}+\Gamma^{1}_{a}\Gamma^{2}_{b}-\Gamma^{2}_{a}\Gamma^{1}_{b})+E^{a}_{2}E^{b}_{3}(2\partial_{[a}\Gamma^{1}_{b]}+\Gamma^{2}_{a}\Gamma^{3}_{b}\\ &\quad -\Gamma^{3}_{a}\Gamma^{2}_{b})+E^{a}_{3}E^{b}_{1}(2\partial_{[a}\Gamma^{2}_{b]}+\Gamma^{3}_{a}\Gamma^{1}_{b}-\Gamma^{1}_{a}\Gamma^{3}_{b})]\\ &= -\frac{2}{\sqrt{\det(E)}}[(E^{a}_{1}E^{\varphi}_{2}-E^{a}_{2}E^{\varphi}_{1})\partial_{a}\Gamma^{3}_{\varphi}+E^{a}_{1}E^{b}_{2}(\Gamma^{1}_{a}\Gamma^{2}_{b}-\Gamma^{2}_{a}\Gamma^{1}_{b})-E^{a}_{2}E^{r}_{3}\partial_{r}\Gamma^{1}_{a}+E^{a}_{1}E^{r}_{3}\partial_{r}\Gamma^{2}_{a}]\\ &= -\frac{2}{\sqrt{\det(E)}}[2E^{[\theta}_{1}E^{\varphi]}_{2}\partial_{\theta}\Gamma^{3}_{\varphi}+4E^{[\theta}_{1}E^{\varphi]}_{2}\Gamma^{1}_{[\theta}\Gamma^{2}_{\varphi]}-E^{\theta}_{2}E^{r}_{3}\partial_{r}\Gamma^{1}_{\theta}-E^{\varphi}_{2}E^{r}_{3}\partial_{r}\Gamma^{1}_{\varphi}+E^{\theta}_{1}E^{r}_{3}\partial_{r}\Gamma^{2}_{\theta}+E^{\varphi}_{1}E^{r}_{3}\partial_{r}\Gamma^{2}_{\varphi}].\end{aligned} \tag{A11}$$

For our purposes, we can further simplify Eq. (A11) by using the following relations which are due to spherical symmetry:

$$\begin{aligned}E^{\theta}_{1} &= \sin\theta E^{\varphi}_{2}, \qquad E^{\theta}_{2} = -\sin\theta E^{\varphi}_{1},\\ \Gamma^{1}_{\varphi} &= -\sin\theta\Gamma^{2}_{\theta}, \qquad \Gamma^{2}_{\varphi} = \sin\theta\Gamma^{1}_{\theta}.\end{aligned} \tag{A12}$$

We shall use these equations everywhere except for the fluxes that are acted on by ∂_{θ}. Doing this, we find

$$\begin{aligned}\sqrt{\det(E)}R &= -\frac{2}{\sqrt{\sin\theta E^{r}_{3}[(E^{\varphi}_{1})^{2}+(E^{\varphi}_{2})^{2}]}}[\sin\theta[(E^{\varphi}_{1})^{2}+(E^{\varphi}_{2})^{2}]\partial_{\theta}\Gamma^{3}_{\varphi}\\ &\quad +\sin^{2}\theta[(E^{\varphi}_{1})^{2}+(E^{\varphi}_{2})^{2}][(\Gamma^{1}_{\theta})^{2}+(\Gamma^{2}_{\theta})^{2}]+2\sin\theta E^{r}_{3}E^{\varphi}_{1}\partial_{r}\Gamma^{1}_{\theta}+2\sin\theta E^{\varphi}_{2}E^{r}_{3}\partial_{r}\Gamma^{2}_{\theta}]\\ &= -\frac{2}{\sqrt{\sin\theta E^{r}_{3}[(E^{\varphi}_{1})^{2}+(E^{\varphi}_{2})^{2}]}}[\sin\theta[(E^{\varphi}_{1})^{2}+(E^{\varphi}_{2})^{2}](\partial_{\theta}\Gamma^{3}_{\varphi}\\ &\quad +\sin\theta[(\Gamma^{1}_{\theta})^{2}+(\Gamma^{2}_{\theta})^{2}])+2\sin\theta E^{r}_{3}(E^{\varphi}_{1}\partial_{r}\Gamma^{1}_{\theta}+E^{\varphi}_{2}\partial_{r}\Gamma^{2}_{\theta})].\end{aligned} \tag{A13}$$

We now eliminate Γ^i_a in favor of E^a_i and its derivatives. By definition we have

$$\Gamma^j_b = -\frac{1}{2}\epsilon^{jik}E^a_k\left[E^i_{b,a} - E^i_{a,b} + E^c_i E^l_b E^l_{c,a} + E^i_b\frac{\det(E)_{,a}}{\det(E)} - \frac{1}{2}E^i_a\frac{\det(E)_{,b}}{\det(E)}\right], \tag{A14}$$

with

$$E^i_a = \frac{1}{2\det(E)}\epsilon_{abc}\epsilon^{ijk}E^b_j E^c_k. \tag{A15}$$

For Γ^i_θ and Γ^3_φ we find

$$\begin{aligned}
\Gamma^3_\varphi &= -\frac{1}{2}E^\theta_2[E^1_{\varphi,\theta} + E^\theta_1(E^1_\varphi E^1_{\theta,\theta} + E^2_\varphi E^2_{\theta,\theta}) + E^\varphi_1(E^1_\varphi E^1_{\varphi,\theta} + E^2_\varphi E^2_{\varphi,\theta}) \\
&\quad + E^1_\varphi \log[\det(E)]_{,\theta}] + \frac{1}{2}E^\theta_1[E^2_{\varphi,\theta} + E^\theta_2(E^1_\varphi E^1_{\theta,\theta} + E^2_\varphi E^2_{\theta,\theta}) + E^\varphi_2(E^1_\varphi E^1_{\varphi,\theta} \\
&\quad + E^2_\varphi E^2_{\varphi,\theta}) + E^2_\varphi \log[\det(E)]_{,\theta}] \\
&= -\frac{1}{2E^r_3(E^\theta_2E^\varphi_1 - E^\theta_1E^\varphi_2)^2}[-(E^\theta_1)^3E^\varphi_2E^r_{3,\theta} + (E^\theta_1)^2(E^\theta_2E^\varphi_1E^r_{3,\theta} - E^r_3 \\
&\quad \times [E^\varphi_2E^\theta_{1,\theta} + E^\varphi_1E^\theta_{2,\theta}]) + (E^\theta_2)^2(E^\theta_2E^\varphi_1E^r_{3,\theta} + E^r_3[E^\varphi_2E^\theta_{1,\theta} + E^\varphi_1E^\theta_{2,\theta}]) \\
&\quad - E^\theta_1E^\theta_2(E^\theta_2E^\varphi_2E^r_{3,\theta} + 2E^r_3[-E^\varphi_1E^\theta_{1,\theta} + E^\varphi_2E^\theta_{2,\theta}])] \\
&= -\frac{1}{2(E^r_3)^2[(E^\varphi_1)^2 + (E^\varphi_2)^2]^2}\left[-\frac{2(E^r_3)^2}{\sin\theta}(E^\varphi_1E^\theta_{1,\theta} + E^\varphi_2E^\theta_{2,\theta})^2 + \sin\theta[(E^\varphi_1)^2\right. \\
&\quad + (E^\varphi_2)^2]^2[(E^r_{3,\theta})^2 - E^r_3E^r_{3,\theta\theta}] + E^r_3[(E^\varphi_1)^2 + (E^\varphi_2)^2](-E^\varphi_2[E^r_{3,\theta}E^\theta_{1,\theta} + E^r_3E^\theta_{1,\theta\theta}] \\
&\quad \left. + E^\varphi_1[E^r_{3,\theta}E^\theta_{2,\theta} + E^r_3E^\theta_{2,\theta\theta}])\right],
\end{aligned} \tag{A16a}$$

$$\begin{aligned}
\Gamma^1_\theta &= -\frac{1}{2}E^r_3[E^2_{\theta,r} + E^\theta_2(E^1_\theta E^1_{\theta,r} + E^2_\theta E^2_{\theta,r}) + E^\varphi_2(E^1_\theta E^1_{\varphi,r} + E^2_\theta E^2_{\varphi,r}) \\
&\quad + E^2_\theta \log[\det(E)]_{,r}] \\
&= -\frac{1}{2(E^\theta_2E^\varphi_1 - E^\theta_1E^\varphi_2)^2}[E^\varphi_1E^r_{3,r}(E^\theta_2E^\varphi_1 - E^\theta_1E^\varphi_2) + E^r_3(E^\theta_1[-E^\varphi_2E^\varphi_{1,r} \\
&\quad + E^\varphi_1E^\varphi_{2,r}] + E^\theta_2[E^\varphi_1E^\varphi_{1,r} + E^\varphi_2E^\varphi_{2,r}] - E^\theta_{2,r}[(E^\varphi_1)^2 + (E^\varphi_2)^2])] \\
&= \frac{E^\varphi_1E^r_{3,r}}{2\sin\theta[(E^\varphi_1)^2 + (E^\varphi_2)^2]}
\end{aligned} \tag{A16b}$$

$$\begin{aligned}
\Gamma^2_\theta &= \frac{1}{2}E^r_3[E^1_{\theta,r} + E^\theta_1(E^1_\theta E^1_{\theta,r} + E^2_\theta E^2_{\theta,r}) + E^\varphi_1(E^1_\theta E^1_{\varphi,r} + E^2_\theta E^2_{\varphi,r}) \\
&\quad + E^1_\theta \log[\det(E)]_{,r}] \\
&= -\frac{1}{2(E^\theta_2E^\varphi_1 - E^\theta_1E^\varphi_2)^2}[E^\varphi_2E^r_{3,r}(E^\theta_2E^\varphi_1 - E^\theta_1E^\varphi_2) + E^r_3(E^\theta_2[-E^\varphi_2E^\varphi_{1,r} \\
&\quad + E^\varphi_1E^\varphi_{2,r}] - E^\theta_1[E^\varphi_1E^\varphi_{1,r} + E^\varphi_2E^\varphi_{2,r}] + E^\theta_{1,r}[(E^\varphi_1)^2 + (E^\varphi_2)^2])] \\
&= \frac{E^\varphi_2E^r_{3,r}}{2\sin\theta[(E^\varphi_1)^2 + (E^\varphi_2)^2]}.
\end{aligned} \tag{A16c}$$

In Eq. (A16) we used $\partial_\theta E^\varphi_i = 0$ as suggested by spherical symmetry. Using the above, Eq. (A13) reduces to

$$\begin{aligned}\sqrt{\det(E)}R = &-\frac{1}{2(E^r_3)^{5/2}\sin^{1/2}\theta[(E^\varphi_1)^2+(E^\varphi_2)^2]^{3/2}}[-2\sin^2\theta(E^\varphi_1)^4[(\partial_\theta E^r_3)^2 - E^r_3\partial^2_\theta E^r_3]\\ &- 2\sin\theta E^r_3(E^\varphi_1)^3[\partial_\theta E^r_3\partial_\theta E^\theta_2 + E^r_3\partial^2_\theta E^\theta_2] - 2E^r_3E^\varphi_1(E^\varphi_2[(\sin\theta E^\varphi_2\partial_\theta E^r_3 - 4E^r_3\partial_\theta E^\theta_1)\partial_\theta E^\theta_2\\ &+ \sin\theta E^r_3E^\varphi_2\partial^2_\theta E^\theta_2] + 2(E^r_3)^2\partial_r E^\varphi_1\partial_r E^r_3) + (E^\varphi_1)^2(-4\sin^2\theta(E^\varphi_2)^2[(\partial_\theta E^r_3)^2 - E^r_3\partial^2_\theta E^r_3]\\ &+ 2\sin\theta E^r_3E^\varphi_2[\partial_\theta E^r_3\partial_\theta E^\theta_1 + E^r_3\partial^2_\theta E^\theta_1] + (E^r_3)^2[4(\partial_\theta E^\theta_1)^2 + (\partial_r E^r_3)^2 + 4E^r_3\partial^2_r E^r_3]) + E^\varphi_2(-2\sin^2\theta\\ &\times(E^\varphi_2)^3[(\partial_\theta E^r_3)^2 - E^r_3\partial^2_\theta E^r_3] + 2\sin\theta E^r_3(E^\varphi_2)^2[\partial_\theta E^r_3\partial_\theta E^\theta_1 + E^r_3\partial^2_\theta E^\theta_1] - 4(E^r_3)^3\partial_r E^\varphi_2\partial_r E^r_3 + (E^r_3)^2E^\varphi_2\\ &\times[4(\partial_\theta E^\theta_2)^2 + (\partial_r E^r_3)^2 + 4E^r_3\partial^2_r E^r_3])]. \end{aligned} \tag{A17}$$

APPENDIX B: COHERENT STATES

The derivation of Eq. (91) is straightforward given that only τ_3 appears. Let us then show how we arrive at Eqs. (92) and (93) by providing a few more details. First of all, given the property $u^{-1}_\ell\tau_\ell u_\ell = \tau_3$ and the relations given in Eq. (53), we have

$$\begin{aligned}\tau_x &= \tau_1\cos\tilde{\alpha} + \tau_2\sin\tilde{\alpha},\\ \tau_y &= -\tau_1\sin\tilde{\alpha} + \tau_2\cos\tilde{\alpha},\\ \tau_1 &= \tau_x\cos\tilde{\alpha} - \tau_y\sin\tilde{\alpha},\\ \tau_2 &= \tau_x\sin\tilde{\alpha} + \tau_y\cos\tilde{\alpha},\end{aligned}$$

from which

$$E^1\tau_1 + E^2\tau_2 = E\tau_x, \tag{B1}$$

$$E^1\tau_2 - E^2\tau_1 = E\tau_y, \tag{B2}$$

with $E = \Lambda R$. Notice that we have expressed the relation between the internal directions (1,2) and (x, y) in terms of the angle $\tilde{\alpha}$ since we are interested in the classical solution for the triad and connection to define the $SL(2,\mathbb{C})$ group elements around which the semiclassical states are peaked. It follows that for the coherent state along the θ-direction we have

$$\begin{aligned}&{}^xD^{j_x}_{\tilde{n}_x\tilde{m}_x}\big(e^{\epsilon_\theta(A_1\tau_1+A_2\tau_2)}e^{\frac{\lambda\delta^2_\theta}{\kappa\gamma}(E^1\tau_1+E^2\tau_2)\sin\theta}\big)\\ &\quad= D^{j_x}_{\tilde{n}_x\tilde{m}_x}\big(u^{-1}_x e^{\epsilon_\theta(A_1\tau_1+A_2\tau_2)}e^{\frac{\lambda\delta^2_\theta}{\kappa\gamma}E\tau_x\sin\theta}u_x\big)\\ &\quad= e^{\lambda\tilde{m}_x\frac{\delta^2_\theta E^x}{\kappa\gamma}x}D^{j_x}_{\tilde{n}_x\tilde{m}_x}\big(e^{\epsilon_\theta(A_1\tau_1+A_2\tau_2)}\big)\end{aligned} \tag{B3}$$

where $E^x = E\sin\theta$.

Similarly, for the coherent state along the φ-direction we have

$$\begin{aligned}&{}^yD^{j_y}_{\tilde{n}_y\tilde{m}_y}\big(e^{\epsilon_\varphi[(A_1\tau_2-A_2\tau_1)\sin\theta+\cos\theta\tau_3]}e^{\frac{\lambda\delta^2_\varphi}{\kappa\gamma}(E^1\tau_2-E^2\tau_1)}\big)\\ &\quad= e^{\lambda\tilde{m}_y\frac{\delta^2_\varphi E^y}{\kappa\gamma}y}D^{j_y}_{\tilde{n}_y\tilde{m}_y}\big(e^{\epsilon_\varphi[(A_1\tau_2-A_2\tau_1)\sin\theta+\cos\theta\tau_3]}\big),\end{aligned} \tag{B4}$$

where $E^y = E$.

APPENDIX C: APPROXIMATING THE LORENTZIAN HAMILTONIAN VIA TECHNIQUES OF REGGE CALCULUS

In this Appendix we provide an alternative method for quantizing the Lorentzian part of the Hamiltonian constraint.

As we noted in Sec. III, the Lorentzian term can be written either in terms of the extrinsic curvature or in terms of the 3D Ricci scalar as we do so in Eq. (31). In [145] a proposal was introduced aiming at providing an alternative approach to Thiemann's construction [105] for quantizing the Lorentzian term. The advantage of this approach is that it is computationally straightforward. Nonetheless, this approach is inherently "perturbative" as will become clear below. In situations where nonperturbative quantum gravity effects are likely to be influential (e.g., black hole singularity resolution), this approach may fall short of providing both the correct qualitative and quantitative pictures. Nevertheless, we now briefly review the regularization scheme of [145] and then describe how the Lorentzian part of the Hamiltonian constraint can be quantized in our framework, using this approach.

The main idea behind the construction of [145] is to regularize the integral of the Ricci scalar over Σ_t by means of Regge calculus [146], i.e., in terms of lengths and angles of the triangulation. More precisely, assuming that curvature lies only on the hinges h of the simplicial decomposition Δ of the 3D manifold Σ, we have the simplicial approximation

$$\frac{1}{2}\int_\Delta\sqrt{\det(E)}R = \sum_s\sum_{h\in s}L^s_h\left(\frac{2\pi}{\alpha_h} - \theta^s_h\right), \tag{C1}$$

where the first sum is over the simplices s of Δ and the second one is over the hinges in the given simplex. The geometrical quantity L^s_h represents the length of the hinge h in the simplex s, θ^s_h is the dihedral angle at the hinge h, and α_h is the number of simplices sharing the hinge h. The continuum limit can be obtained by sending the typical length of the lattice to zero and the construction

can be straightforwardly generalized to nonsimplicial decompositions, as long as the hinges are straight lines.[15]

Let us focus on a 3-valent vertex v of our cuboidal decomposition. The three edges in the directions r,θ,φ emanating from the vertex v represent the three hinges on which the curvature is concentrated (see Fig. 2). The lengths of these three hinges are given respectively by

$$L_r = \frac{\sqrt{\epsilon_i{}^{jk}E_j(S^\theta)E_k(S^\varphi)\epsilon^{ilm}E_l(S^\theta)E_m(S^\varphi)}}{V(v)} = \frac{|E(S^\theta)||E(S^\varphi)|}{V(v)}, \tag{C2a}$$

$$L_\theta = \frac{\sqrt{\epsilon_i{}^{jk}E_j(S^r)E_k(S^\varphi)\epsilon^{ilm}E_l(S^r)E_m(S^\varphi)}}{V(v)} = \frac{|E(S^r)||E(S^\varphi)|}{V(v)}, \tag{C2b}$$

$$L_\varphi = \frac{\sqrt{\epsilon_i{}^{jk}E_j(S^r)E_k(S^\theta)\epsilon^{ilm}E_l(S^r)E_m(S^\theta)}}{V(v)} = \frac{|E(S^r)||E(S^\theta)|}{V(v)}. \tag{C2c}$$

Here the flux $E_i(S^a)$ is defined in Eq. (44). The corresponding dihedral angles are

$$\theta_r = \pi - \arccos\left[\frac{\delta^{ij}E_i(S^\theta[x_1])E_j(S^\varphi[x_2])}{|E(S^\theta)||E(S^\varphi)|}\right], \tag{C3a}$$

$$\theta_\theta = \pi - \arccos\left[\frac{\delta^{ij}E_i(S^r[x_1])E_j(S^\varphi[x_2])}{|E(S^r)||E(S^\varphi)|}\right], \tag{C3b}$$

$$\theta_\varphi = \pi - \arccos\left[\frac{\delta^{ij}E_i(S^r[x_1])E_j(S^\theta[x_2])}{|E(S^r)||E(S^\theta)|}\right], \tag{C3c}$$

where $|E(S^a)| = \sqrt{\delta^{ij}E_i(S^a)E_j(S^a)}$. We promote the right-hand side of Eq. (C1) to an operator by replacing the classical length and angle variables by their quantum counterparts. Now the expectation value of the quantum version of the right-hand side of Eq. (C1) on the semiclassical states is simply given by the classical expression described below.

To compute the right-hand side of Eq. (C1), we need the following expansion in terms of the holonomies of spin connections:

[15]In particular to the case of a cuboidal triangulation which we are interested in.

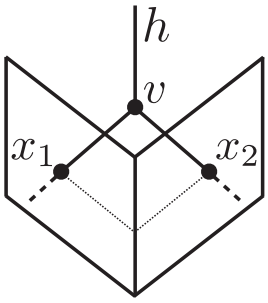

FIG. 2. Intersection of the graph with the dual surfaces where the fluxes are evaluated in order to compute the dihedral angle around the hinge h.

$$E_i(S^a[x_1])E_j(S^b[x_2]) = E_i(S^a[v])[\delta^l_j - \epsilon^a\epsilon^b\epsilon_{jk}{}^lR^k_{ab}(v)] \times E_l(S^b[v]) + o(\epsilon^3). \tag{C4}$$

On the left-hand side of the expression above, the two fluxes that read the dihedral angle around the hinge h are not computed at the same point. They intersect the dual links (the edges of the graph) away from the vertex v, at two points x_1 and x_2. On the right-hand side we have expressed their product in terms of the fluxes evaluated at the same point v times the parallel transport through holonomies of the intrinsic curvature Γ^i_a from x_1 and x_2 to v. Such parallel transport can be written as a Wilson loop on the plane dual to the hinge and thus expressed in terms of the curvature of Γ^i_a.

It is immediate to see that the zeroth order in ϵ inside the arccos function vanishes, since the fluxes are orthogonal, and thus the leading order gives a $o(\epsilon^2)$ term.

The contribution of a single 3-valent vertex to the integral of the Ricci scalar is hence given by (considering that each hinge is shared by four cubes)

$$\sum_{a=r,\theta,\varphi} L_a\left(\frac{\pi}{2}-\theta_a\right) = L_r\frac{(E_2(S^\theta)E_1(S^\varphi) - E_1(S^\theta)E_2(S^\varphi))R^3_{\theta\varphi}\epsilon_\theta\epsilon_\varphi}{|E(S^\theta)||E(S^\varphi)|} + L_\theta\frac{E_3(S^r)(E_2(S^\varphi)R^1_{r\varphi} - E_1(S^\varphi)R^2_{r\varphi})\epsilon_r\epsilon_\varphi}{|E(S^r)||E(S^\varphi)|} + L_\varphi\frac{E_3(S^r)(E_2(S^\theta)R^1_{r\theta} - E_1(S^\theta)R^2_{r\theta})\epsilon_r\epsilon_\theta}{|E(S^r)||E(S^\theta)|}. \tag{C5}$$

By means of Eqs. (C2) and (A3), and the relation $E^a_i = \sqrt{\det(E)}e^a_i$, it is straightforward to check that

$$\sum_{a=r,\theta,\varphi} L_a\left(\frac{\pi}{2}-\theta_a\right) = \epsilon_r\epsilon_\theta\epsilon_\varphi\sqrt{\det(E)}[(e^\theta_2e^\varphi_1 - e^\theta_1e^\varphi_2)R^3_{\theta\varphi} + e^r_3(e^\varphi_2R^1_{r\varphi} - e^\varphi_1R^2_{r\varphi}) + e^r_3(e^\theta_2R^1_{r\theta} - e^\theta_1R^2_{r\theta})] = \epsilon_r\epsilon_\theta\epsilon_\varphi\sqrt{\det(E)}R, \tag{C6}$$

as expected.

1. Higher order holonomy correction to the triangulation formula for total curvature

Equation (C4) contains the first nontrivial correction due to the curvature. Here we derive the next order correction. From the derivation of [147], we have

$$E_i(S^a[x_1])E_j(S^b[x_2]) = E_i(S^a[v])[\delta^l{}_j + R^l{}_{jab}\epsilon^a\epsilon^b + \frac{1}{2}R^l{}_{jab;a}\epsilon^{a2}\epsilon^b + \frac{1}{2}R^l{}_{jab;b}\epsilon^a\epsilon^{b2}]E_l(S^b[v]) + o(\epsilon^4). \tag{C7}$$

For the length-angle formula, the first term in the square bracket does not contribute. The contribution of the second term was worked out above. Here we focus on the third and fourth terms.

Note that since total curvature is invariant under arbitrary spatial diffeomorphisms, the final result of this calculation cannot depend on the internal angle α. Therefore, for simplicity and to reduce the number of expressions we set $\alpha = 0$ at the vertex v. This way $e^\varphi_1 = e^\theta_2 = 0$ at v. The nonvanishing holonomy corrections are

$$\begin{aligned}
E_1(S^\theta[x_1])E_1(S^\varphi[x_2])|_{\epsilon^3} &= \frac{\epsilon^\theta\epsilon^\varphi}{2}E_1(S^\theta)E_2(S^\varphi)[R^2{}_{1\theta\varphi;\theta}\epsilon^\theta + R^2{}_{1\theta\varphi;\varphi}\epsilon^\varphi],\\
E_3(S^r[x_1])E_3(S^\varphi[x_2])|_{\epsilon^3} &= \frac{\epsilon^r\epsilon^\varphi}{2}E_3(S^r)E_2(S^\varphi)[R^2{}_{3r\varphi;r}\epsilon^r + R^2{}_{3r\varphi;\varphi}\epsilon^\varphi],\\
E_3(S^r[x_1])E_3(S^\theta[x_2])|_{\epsilon^3} &= \frac{\epsilon^r\epsilon^\theta}{2}E_3(S^r)E_1(S^\theta)[R^1{}_{3r\theta;r}\epsilon^r + R^1{}_{3r\theta;\theta}\epsilon^\theta].
\end{aligned} \tag{C8}$$

The correction to the length-angle term becomes

$$\begin{aligned}
\sum_{a=r,\theta,\varphi} L_a\left(\frac{\pi}{2}-\theta_a\right)\Big|_{\epsilon^4} &= -\frac{\epsilon^r\epsilon^\theta\epsilon^\varphi}{2}\sqrt{\det(E)}[e^\theta_1 e^\varphi_2(R^2{}_{1\theta\varphi;\theta}\epsilon^\theta + R^2{}_{1\theta\varphi;\varphi}\epsilon^\varphi)\\
&\quad + e^r_3 e^\varphi_2(R^2{}_{3r\varphi;r}\epsilon^r + R^2{}_{3r\varphi;\varphi}\epsilon^\varphi) + e^r_3 e^\theta_1(R^1{}_{3r\theta;r}\epsilon^r + R^1{}_{3r\theta;\theta}\epsilon^\theta)]\\
&= -\frac{\epsilon^r\epsilon^\theta\epsilon^\varphi}{2}\sqrt{\det(E)}[\epsilon^\theta(e^\theta_1 e^\varphi_2 R^2{}_{1\theta\varphi;\theta} + e^\theta_1 e^r_3 R^1{}_{3r\theta;\theta})\\
&\quad + \epsilon^\varphi(e^\varphi_2 e^\theta_1 R^2{}_{1\theta\varphi;\varphi} + e^\varphi_2 e^r_3 R^2{}_{3r\varphi;\varphi}) + \epsilon^r(e^r_3 e^\theta_1 R^1{}_{3r\theta;r} + e^r_3 e^\varphi_2 R^2{}_{3r\varphi;r})]\\
&= -\frac{\epsilon^r\epsilon^\theta\epsilon^\varphi}{2}\sqrt{\det(E)}[\epsilon^\theta(R^2{}_{112;\theta} + R^1{}_{331;\theta} - R^2{}_{11\varphi}e^\varphi_{2;\theta} - R^2{}_{1\theta2}e^\theta_{1;\theta}\\
&\quad - R^1{}_{3r1}e^r_{3;\theta} - R^1{}_{33\theta}e^\theta_{1;\theta}) + \epsilon^\varphi(R^2{}_{112;\varphi} + R^2{}_{332;\varphi} - R^2{}_{11\varphi}e^\varphi_{2;\varphi}\\
&\quad - R^2{}_{1\theta2}e^\theta_{1;\varphi} - R^2{}_{33\varphi}e^\varphi_{2;\varphi} - R^2{}_{3r2}e^r_{3;\varphi}) + \epsilon^r(R^1{}_{331;r} + R^2{}_{332;r}\\
&\quad - R^1{}_{3r1}e^r_{3;r} - R^1{}_{33\theta}e^\theta_{1;r} - R^2{}_{3r2}e^r_{3;r} - R^2{}_{33\varphi}e^\varphi_{2;r})].
\end{aligned} \tag{C9}$$

We can simplify the above expression by noting that

$$\begin{aligned}
e^\varphi_{2;\theta} &= e^\varphi_{2,\theta} + \Gamma^\varphi_{\varphi\theta}e^\varphi_2 = -\frac{1}{R\sin\theta}\cot\theta + \frac{1}{R\sin\theta}\cot\theta = 0,\\
e^\theta_{1;\theta} &= e^r_{3;\theta} = e^\varphi_{2;\varphi} = e^\theta_{1;\varphi} = e^r_{3;\varphi} = 0,\\
e^r_{3;r} &= e^r_{3,r} + \Gamma^r_{rr}e^r_3 = -\frac{\Lambda'}{\Lambda 2} + \frac{\Lambda'}{\Lambda 2} = 0,\\
e^\theta_{1;r} &= e^\theta_{1,r} + \Gamma^\theta_{\theta r}e^\theta_1 = -\frac{R'}{R^2} + \frac{R'}{R^2} = 0,\\
e^\varphi_{2;r} &= e^\varphi_{2,r} + \Gamma^\varphi_{\varphi r}e^\varphi_2 = -\frac{R'}{R^2\sin\theta} + \frac{R'}{R^2\sin\theta} = 0.
\end{aligned} \tag{C10}$$

Thus, (C9) becomes

$$\sum_{a=r,\theta,\varphi} L_a\left(\frac{\pi}{2}-\theta_a\right)\Big|_{\epsilon^4} = -\frac{\epsilon^r\epsilon^\theta\epsilon^\varphi}{2}\sqrt{\det(E)}[\epsilon^\theta(R^2{}_{112;\theta}+R^1{}_{331;\theta})+\epsilon^\varphi(R^2{}_{112;\varphi}+R^2{}_{332;\varphi})+\epsilon^r(R^1{}_{331;r}+R^2{}_{332;r})]. \quad \text{(C11)}$$

It follows from symmetries of the Riemann tensor and the definition of the internal metric that

$$\begin{aligned} &R^2{}_{112} = R_{2112} = -R_{1212}, \qquad R^1{}_{331} = R_{1331} = -R_{1313},\\ &R^2{}_{332} = R_{2332} = -R_{2323},\\ &R_{1212}+R_{1313} = R_{11}, \qquad R_{1212}+R_{3232} = R_{22},\\ &R_{1313}+R_{2323} = R_{33}. \end{aligned} \quad \text{(C12)}$$

Therefore, (C11) reduces to

$$\sum_{a=r,\theta,\varphi} L_a\left(\frac{\pi}{2}-\theta_a\right)\Big|_{\epsilon^4} = \frac{\epsilon^r\epsilon^\theta\epsilon^\varphi}{2}\sqrt{\det(E)}[\epsilon^\theta R_{11;\theta}+\epsilon^\varphi R_{22;\varphi}+\epsilon^r R_{33;r}]. \quad \text{(C13)}$$

Due to spherical symmetry we have

$$\begin{aligned} R_{11;\theta} &= e_1^{\theta 2}R_{\theta\theta;\theta} = e_1^{\theta 2}R_{\theta\theta,\theta} = 0,\\ R_{22;\varphi} &= e_2^{\varphi 2}R_{\varphi\varphi;\varphi} = e_2^{\varphi 2}R_{\varphi\varphi,\varphi} = 0,\\ R_{33;r} &= e_3^{r2}R_{rr;r} = e_3^{r2}[R_{rr,r}-2\Gamma^r_{rr}R_{rr}] = \frac{2}{R^2\Lambda^4}[-3RR'\Lambda'^2\\ &\quad +\Lambda(-\Lambda'[R'^2-3RR'']+RR'\Lambda'')+\Lambda^2(R'R''-RR''')]. \end{aligned} \quad \text{(C14)}$$

Putting everything together, (C13) reduces to

$$\begin{aligned} \sum_{a=r,\theta,\varphi} L_a\left(\frac{\pi}{2}-\theta_a\right)\Big|_{\epsilon^4} &= \frac{(\epsilon^r)^2\epsilon^\theta\epsilon^\varphi}{2}\sqrt{\det(E)}R_{33;r}\\ &= (\epsilon^r)^2\epsilon^\theta\epsilon^\varphi\frac{\sin\theta}{\Lambda^3}[-3RR'\Lambda'^2+\Lambda(-\Lambda'[R'^2-3RR'']+RR'\Lambda'')+\Lambda^2(R'R''-RR''')]. \end{aligned} \quad \text{(C15)}$$

That this result is somewhat different from what was obtained in Eq. (114) is not all that surprising. Indeed the method here and the one is Sec. VII B correspond to two different regularization schemes for the spin connections.

[1] R. Penrose, Gravitational Collapse and Space-Time Singularities, Phys. Rev. Lett. **14**, 57 (1965).
[2] E. M. Lifshitz and I. M. Khalatnikov, Investigations in relativistic cosmology, Adv. Phys. **12**, 185 (1963).
[3] J. R. Oppenheimer and H. Snyder, On continued gravitational contraction, Phys. Rev. **56**, 455 (1939).
[4] S. Hawking, The occurrence of singularities in cosmology. III. Causality and singularities, Proc. R. Soc. A **300**, 187 (1967).
[5] S. Hawking, The singularities of gravitational collapse and cosmology, Proc. R. Soc. A **314**, 529 (1970).
[6] S. W. Hawking and G. F. R. Ellis, *The Large Scale Structure of Space-Time*, Cambridge Monographs on Mathematical Physics (Cambridge University Press, Cambridge, England, 2011).
[7] R. Penrose, Singularities and time-asymmetry, in *General Relativity: An Einstein Centenary Survey* (University Press, Cambridge, 1979), pp. 581–638.
[8] J. H. Christenson, J. W. Cronin, V. L. Fitch, and R. Turlay, Evidence for the 2π Decay of the k_2^0 Meson, Phys. Rev. Lett. **13**, 138 (1964).
[9] R. C. Casella, Time Reversal and the K^0 Meson Decays, Phys. Rev. Lett. **21**, 1128 (1968).
[10] L. Wolfenstein, Violation of CP Invariance and the Possibility of Very Weak Interactions, Phys. Rev. Lett. **13**, 562 (1964).

[11] S. Hawking and R. Penrose, *The Nature of Space and Time (New in Paper)* (Princeton University Press, Princeton, NJ, 1996).
[12] P. J. Steinhardt and N. Turok, The cyclic universe: An informal introduction, Nucl. Phys. B, Proc. Suppl. **124**, 38 (2003).
[13] P. J. Steinhardt and N. Turok, The cyclic model simplified, New Astron. Rev. **49**, 43 (2005).
[14] R. Penrose, Gravitational collapse: The role of general relativity, Riv. Nuovo Cimento **1**, 252 (1969).
[15] S. W. Hawking, Particle creation by black holes, Commun. Math. Phys. **43**, 199 (1975).
[16] J. Preskill, Do black holes destroy information?, in *An international symposium on Black Holes, Membranes, Wormholes and Superstrings, Houston Advanced Research Center, 1992*, edited by Sunny Kalara and D. V. Nanopoulos (World Scientific, Singapore, 1993), pp. 22–39.
[17] A. Almheiri, D. Marolf, J. Polchinski, and J. Sully, Black holes: Complementarity or firewalls?, J. High Energy Phys. 2 (2013) 62.
[18] S. D. Mathur, The fuzzball proposal for black holes: An elementary review, Fortschr. Phys. **53**, 793 (2005).
[19] Y. Aharonov, A. Casher, and S. Nussinov, The unitarity puzzle and Planck mass stable particles, Phys. Lett. B **191**, 51 (1987).
[20] S. B. Giddings, Black holes and massive remnants, Phys. Rev. D **46**, 1347 (1992).
[21] A. Ashtekar and M. Bojowald, Black hole evaporation: A paradigm, Classical Quantum Gravity **22**, 3349 (2005).
[22] T. Banks, M. O'Loughlin, and A. Strominger, Black hole remnants and the information puzzle, Phys. Rev. D **47**, 4476 (1993).
[23] S. B. Giddings, Comments on information loss and remnants, Phys. Rev. D **49**, 4078 (1994).
[24] S. Hossenfelder and L. Smolin, Conservative solutions to the black hole information problem, Phys. Rev. D **81**, 064009 (2010).
[25] A. Perez, No firewalls in quantum gravity: The role of discreteness of quantum geometry in resolving the information loss paradox, Classical Quantum Gravity **32**, 084001 (2015).
[26] G. T. Horowitz and S. F. Ross, Possible resolution of black hole singularities from large N gauge theory, J. High Energy Phys. 04 (1998) 015.
[27] B. Craps, T. Hertog, and N. Turok, On the quantum resolution of cosmological singularities using AdS/CFT, Phys. Rev. D **86**, 043513 (2012).
[28] N. Turok, B. Craps, and T. Hertog, From big crunch to big bang with AdS/CFT, arXiv:0711.1824.
[29] S. R. Das, J. Michelson, K. Narayan, and S. P. Trivedi, Cosmologies with null singularities and their gauge theory duals, Phys. Rev. D **75**, 026002 (2007).
[30] T. Hertog and G. T. Horowitz, Towards a big crunch dual, J. High Energy Phys. 07 (2004) 073.
[31] E. Silverstein, Invited Talk presented at 23rd Solvay Conference in Physics, in *The Quantum Structure of Space and Time, Brussels, Belgium, 2005* (2006), pp. 70–81.
[32] G. T. Horowitz and E. Silverstein, The inside story: Quasilocal tachyons and black holes, Phys. Rev. D **73**, 064016 (2006).
[33] B. Craps, S. Sethi, and E. P. Verlinde, A matrix big bang, J. High Energy Phys. 10 (2005) 005.
[34] T. Ishino and N. Ohta, Matrix string description of cosmic singularities in a class of time-dependent solutions, Phys. Lett. B **638**, 105 (2006).
[35] L. Cornalba, M. S. Costa, and C. Kounnas, A resolution of the cosmological singularity with orientifolds, Nucl. Phys. **B637**, 378 (2002).
[36] T. Thiemann, *Modern Canonical Quantum General Relativity* (Cambridge University Press, Cambridge, England, 2008).
[37] J. Diaz-Polo and D. Pranzetti, Isolated horizons and black hole entropy in loop quantum gravity, SIGMA **8**, 048 (2012).
[38] A. Perez, Black holes in loop quantum gravity, Rep. Prog. Phys. **80**, 126901 (2017).
[39] L. Modesto, Disappearance of black hole singularity in quantum gravity, Phys. Rev. D **70**, 124009 (2004).
[40] L. Modesto, Loop quantum black hole, Classical Quantum Gravity **23**, 5587 (2006).
[41] A. Ashtekar and M. Bojowald, Quantum geometry and the Schwarzschild singularity, Classical Quantum Gravity **23**, 391 (2006).
[42] C. G. Boehmer and K. Vandersloot, Loop quantum dynamics of the Schwarzschild interior, Phys. Rev. D **76**, 104030 (2007).
[43] M. Campiglia, R. Gambini, and J. Pullin, Loop quantization of spherically symmetric midi-superspaces: The interior problem, AIP Conf. Proc. **977**, 52 (2008).
[44] D.-W. Chiou, Phenomenological loop quantum geometry of the Schwarzschild black hole, Phys. Rev. D **78**, 064040 (2008).
[45] A. Corichi and P. Singh, Loop quantization of the Schwarzschild interior revisited, Classical Quantum Gravity **33**, 055006 (2016).
[46] J. Cortez, W. Cuervo, H. A. Morales-Técotl, and J. C. Ruelas, Effective loop quantum geometry of Schwarzschild interior, Phys. Rev. D **95**, 064041 (2017).
[47] J. Olmedo, S. Saini, and P. Singh, From black holes to white holes: A quantum gravitational, symmetric bounce, Classical Quantum Gravity **34**, 225011 (2017).
[48] A. Ashtekar, M. Bojowald, and J. Lewandowski, Mathematical structure of loop quantum cosmology, Adv. Theor. Math. Phys. **7**, 233 (2003).
[49] A. Ashtekar, Loop quantum cosmology: An overview, Gen. Relativ. Gravit. **41**, 707 (2009).
[50] A. Ashtekar and P. Singh, Loop quantum cosmology: A status report, Classical Quantum Gravity **28**, 213001 (2011).
[51] A. Ashtekar, T. Pawlowski, and P. Singh, Quantum nature of the big bang: An analytical and numerical investigation. I., Phys. Rev. D **73**, 124038 (2006).
[52] A. Ashtekar, T. Pawlowski, and P. Singh, Quantum nature of the big bang: Improved dynamics, Phys. Rev. D **74**, 084003 (2006).
[53] P. Singh, Are loop quantum cosmos never singular?, Classical Quantum Gravity **26**, 125005 (2009).
[54] D. Pranzetti, Radiation from Quantum Weakly Dynamical Horizons in LQG, Phys. Rev. Lett. **109**, 011301 (2012).

[55] D. Pranzetti, Dynamical evaporation of quantum horizons, Classical Quantum Gravity **30**, 165004 (2013).
[56] K. V. Kuchar, Geometrodynamics of Schwarzschild black holes, Phys. Rev. D **50**, 3961 (1994).
[57] T. Thiemann and H. A. Kastrup, Canonical quantization of spherically symmetric gravity in Ashtekar's selfdual representation, Nucl. Phys. **B399**, 211 (1993).
[58] M. Campiglia, R. Gambini, and J. Pullin, Loop quantization of spherically symmetric midi-superspaces, Classical Quantum Gravity **24**, 3649 (2007).
[59] M. Bojowald and H. A. Kastrup, Quantum symmetry reduction for diffeomorphism invariant theories of connections, Classical Quantum Gravity **17**, 3009 (2000).
[60] M. Bojowald and R. Swiderski, The volume operator in spherically symmetric quantum geometry, Classical Quantum Gravity **21**, 4881 (2004).
[61] M. Bojowald and R. Swiderski, Spherically symmetric quantum geometry: Hamiltonian constraint, Classical Quantum Gravity **23**, 2129 (2006).
[62] R. Gambini and J. Pullin, Loop Quantization of the Schwarzschild Black Hole, Phys. Rev. Lett. **110**, 211301 (2013).
[63] R. Gambini, J. Olmedo, and J. Pullin, Quantum black holes in loop quantum gravity, Classical Quantum Gravity **31**, 095009 (2014).
[64] A. Perez, The Spin Foam Approach to Quantum Gravity, Living Rev. Relativity **16**, 3 (2013).
[65] C. Rovelli and F. Vidotto, Planck stars, Int. J. Mod. Phys. A **D23**, 1442026 (2014).
[66] H. M. Haggard and C. Rovelli, Quantum-gravity effects outside the horizon spark black to white hole tunneling, Phys. Rev. D **92**, 104020 (2015).
[67] T. De Lorenzo, C. Pacilio, C. Rovelli, and S. Speziale, On the effective metric of a Planck star, Gen. Relativ. Gravit. **47**, 41 (2015).
[68] S. A. Hayward, Formation and Evaporation of Regular Black Holes, Phys. Rev. Lett. **96**, 031103 (2006).
[69] M. Christodoulou, C. Rovelli, S. Speziale, and I. Vilensky, Planck star tunneling time: An astrophysically relevant observable from background-free quantum gravity, Phys. Rev. D **94**, 084035 (2016).
[70] M. Christodoulou and F. D'Ambrosio, Characteristic time scales for the geometry transition of a black hole to a white hole from spinfoams, arXiv:1801.03027.
[71] A. Barrau and C. Rovelli, Planck star phenomenology, Phys. Lett. B **739**, 405 (2014).
[72] A. Barrau, C. Rovelli, and F. Vidotto, Fast radio bursts and white hole signals, Phys. Rev. D **90**, 127503 (2014).
[73] E. Bianchi, M. Christodoulou, F. D'Ambrosio, C. Rovelli, and H. M. Haggard, White holes as remnants: A surprising scenario for the end of a black hole, arXiv:1802.04264.
[74] D. Oriti, Group field theory as the 2nd quantization of loop quantum gravity, Classical Quantum Gravity **33**, 085005 (2016).
[75] D. Oriti, D. Pranzetti, J. P. Ryan, and L. Sindoni, Generalized quantum gravity condensates for homogeneous geometries and cosmology, Classical Quantum Gravity **32**, 235016 (2015).
[76] D. Oriti, D. Pranzetti, and L. Sindoni, Horizon Entropy from Quantum Gravity Condensates, Phys. Rev. Lett. **116**, 211301 (2016).
[77] D. Oriti, D. Pranzetti, and L. Sindoni, Black holes as quantum gravity condensates, Phys. Rev. D **97**, 066017 (2018).
[78] S. Gielen, D. Oriti, and L. Sindoni, Cosmology from Group Field Theory Formalism for Quantum Gravity, Phys. Rev. Lett. **111**, 031301 (2013).
[79] S. Gielen and D. Oriti, Quantum cosmology from quantum gravity condensates: Cosmological variables and lattice-refined dynamics, New J. Phys. **16**, 123004 (2014).
[80] G. Calcagni, Loop quantum cosmology from group field theory, Phys. Rev. D **90**, 064047 (2014).
[81] D. Oriti, L. Sindoni, and E. Wilson-Ewing, Emergent Friedmann dynamics with a quantum bounce from quantum gravity condensates, Classical Quantum Gravity **33**, 224001 (2016).
[82] M. de Cesare, A. G. A. Pithis, and M. Sakellariadou, Cosmological implications of interacting group field theory models: Cyclic Universe and accelerated expansion, Phys. Rev. D **94**, 064051 (2016).
[83] E. Alesci and F. Cianfrani, A new perspective on cosmology in loop quantum gravity, Europhys. Lett. **104**, 10001 (2013).
[84] E. Alesci and F. Cianfrani, Quantum-reduced loop gravity: Cosmology, Phys. Rev. D **87**, 083521 (2013).
[85] E. Alesci, F. Cianfrani, and C. Rovelli, Quantum-reduced loop-gravity: Relation with the full theory, Phys. Rev. D **88**, 104001 (2013).
[86] E. Alesci and F. Cianfrani, Quantum reduced loop gravity: Semiclassical limit, Phys. Rev. D **90**, 024006 (2014).
[87] E. Alesci and F. Cianfrani, Loop quantum cosmology from quantum reduced loop gravity, Europhys. Lett. **111**, 40002 (2015).
[88] E. Alesci and F. Cianfrani, Quantum reduced loop gravity: Universe on a lattice, Phys. Rev. D **92**, 084065 (2015).
[89] E. Alesci and F. Cianfrani, Quantum reduced loop gravity and the foundation of loop quantum cosmology, Int. J. Mod. Phys. A **D25**, 1642005 (2016).
[90] E. Alesci, G. Botta, F. Cianfrani, and S. Liberati, Cosmological singularity resolution from quantum gravity: The emergent-bouncing universe, Phys. Rev. D **96**, 046008 (2017).
[91] E. Alesci, G. Botta, and G. V. Stagno, Quantum reduced loop gravity effective Hamiltonians from a statistical regularization scheme, Phys. Rev. D **97**, 046011 (2018).
[92] D. M. DeTurck and D. Yang, Existence of elastic deformations with prescribed principal strains and triply orthogonal systems, Duke Math. J. **51**, 243 (1984).
[93] J. D. E. Grant and J. A. Vickers, Block diagonalization of four-dimensional metrics, Classical Quantum Gravity **26**, 235014 (2009).
[94] N. Bodendorfer, J. Lewandowski, and J. Świeżewski, A quantum reduction to spherical symmetry in loop quantum gravity, Phys. Lett. B **747**, 18 (2015).
[95] N. Bodendorfer, J. Lewandowski, and J. Świeżewski, General relativity in the radial gauge: Reduced phase space and canonical structure, Phys. Rev. D **92**, 084041 (2015).

[96] N. Bodendorfer and A. Zipfel, On the relation between reduced quantisation and quantum reduction for spherical symmetry in loop quantum gravity, Classical Quantum Gravity **33**, 155014 (2016).
[97] E. Alesci, C. Pacilio, and D. Pranzetti, Radial gauge fixing of first order gravity, arXiv:1802.06251.
[98] R. L. Arnowitt, S. Deser, and C. W. Misner, The dynamics of general relativity, Gen. Relativ. Gravit. **40**, 1997 (2008).
[99] A. Ashtekar, *New Perspectives in Canonical Gravity* (Napoli, Bibliopolis, 1988), ISBN 88-7088-184-9.
[100] P. Mitra and R. Rajaraman, Gauge invariant reformulation of an anomalous gauge theory, Phys. Lett. B **225**, 267 (1989).
[101] P. Mitra and R. Rajaraman, New results on systems with second class constraints, Ann. Phys. (N.Y.) **203**, 137 (1990).
[102] R. Anishetty and A. S. Vytheeswaran, Gauge invariance in second class constrained systems, J. Phys. A **26**, 5613 (1993).
[103] A. Ashtekar and J. Lewandowski, Background independent quantum gravity: A status report, Classical Quantum Gravity **21**, R53 (2004).
[104] C. Rovelli, *Quantum Gravity*, Cambridge Monographs on Mathematical Physics (Cambridge University Press, Cambridge, England, 2004).
[105] T. Thiemann, Quantum spin dynamics (QSD), Classical Quantum Gravity **15**, 839 (1998).
[106] E. Alesci, M. Assanioussi, J. Lewandowski, and I. Mäkinen, Hamiltonian operator for loop quantum gravity coupled to a scalar field, Phys. Rev. D **91**, 124067 (2015).
[107] E. Alesci, T. Thiemann, and A. Zipfel, Linking covariant and canonical LQG: New solutions to the Euclidean scalar constraint, Phys. Rev. D **86**, 024017 (2012).
[108] E. Alesci, K. Liegener, and A. Zipfel, Matrix elements of Lorentzian Hamiltonian constraint in loop quantum gravity, Phys. Rev. D **88**, 084043 (2013).
[109] C. Rovelli and L. Smolin, Discreteness of area and volume in quantum gravity, Nucl. Phys. **B442**, 593 (1995); Erratum, Nucl. Phys. **B456**, 753(E) (1995).
[110] A. Ashtekar and J. Lewandowski, Quantum theory of geometry. 1: Area operators, Classical Quantum Gravity **14**, A55 (1997).
[111] A. Ashtekar and J. Lewandowski, Quantum theory of geometry. 2. Volume operators, Adv. Theor. Math. Phys. **1**, 388 (1997).
[112] A. Ashtekar, J. Lewandowski, D. Marolf, J. Mourao, and T. Thiemann, Quantization of diffeomorphism invariant theories of connections with local degrees of freedom, J. Math. Phys. (N.Y.) **36**, 6456 (1995).
[113] T. Thiemann and O. Winkler, Gauge field theory coherent states (GCS). 2. Peakedness properties, Classical Quantum Gravity **18**, 2561 (2001).
[114] A. Dasgupta, Semi-classical quantisation of space-times with apparent horizons, Classical Quantum Gravity **23**, 635 (2006).
[115] R. Gambini, E. Mato Capurro, and J. Pullin, Quantum spacetime of a charged black hole, Phys. Rev. D **91**, 084006 (2015).
[116] J. Bilski, E. Alesci, and F. Cianfrani, Quantum reduced loop gravity: Extension to scalar fields, Phys. Rev. D **92**, 124029 (2015).
[117] J. Bilski, E. Alesci, F. Cianfrani, P. Donà, and A. Marciano, Quantum reduced loop gravity: Extension to gauge vector field, Phys. Rev. D **95**, 104048 (2017).
[118] L. Smolin, Linking topological quantum field theory and nonperturbative quantum gravity, J. Math. Phys. (N.Y.) **36**, 6417 (1995).
[119] C. Rovelli, Black Hole Entropy from Loop Quantum Gravity, Phys. Rev. Lett. **77**, 3288 (1996).
[120] K. V. Krasnov, On quantum statistical mechanics of Schwarzschild black hole, Gen. Relativ. Gravit. **30**, 53 (1998).
[121] A. Ashtekar, J. Baez, A. Corichi, and K. Krasnov, Quantum Geometry and Black Hole Entropy, Phys. Rev. Lett. **80**, 904 (1998).
[122] A. Ashtekar, A. Corichi, and K. Krasnov, Isolated horizons: The classical phase space, Adv. Theor. Math. Phys. **3**, 419 (1999).
[123] A. Ashtekar, J. C. Baez, and K. Krasnov, Quantum geometry of isolated horizons and black hole entropy, Adv. Theor. Math. Phys. **4**, 1 (2000).
[124] J. Engle, A. Perez, and K. Noui, Black Hole Entropy and SU(2) Chern-Simons Theory, Phys. Rev. Lett. **105**, 031302 (2010).
[125] J. Engle, K. Noui, A. Perez, and D. Pranzetti, Black hole entropy from an SU(2)-invariant formulation of type I isolated horizons, Phys. Rev. D **82**, 044050 (2010).
[126] A. Perez and D. Pranzetti, Static isolated horizons: SU(2) invariant phase space, quantization, and black hole entropy, Entropy **13**, 744 (2011).
[127] J. Engle, K. Noui, A. Perez, and D. Pranzetti, The SU(2) black hole entropy revisited, J. High Energy Phys. 05 (2011) 016.
[128] E. Frodden, A. Perez, D. Pranzetti, and C. Röken, Modelling black holes with angular momentum in loop quantum gravity, Gen. Relativ. Gravit. **46**, 1828 (2014).
[129] T. Jacobson, Renormalization and black hole entropy in loop quantum gravity, Classical Quantum Gravity **24**, 4875 (2007).
[130] A. Ghosh and A. Perez, Black Hole Entropy and Isolated Horizons Thermodynamics, Phys. Rev. Lett. **107**, 241301 (2011); Erratum, Phys. Rev. Lett. **108**, 169901(E) (2012).
[131] E. Frodden, M. Geiller, K. Noui, and A. Perez, Black hole entropy from complex Ashtekar variables, Europhys. Lett. **107**, 10005 (2014).
[132] A. Ghosh, K. Noui, and A. Perez, Statistics, holography, and black hole entropy in loop quantum gravity, Phys. Rev. D **89**, 084069 (2014).
[133] D. Pranzetti, Geometric temperature and entropy of quantum isolated horizons, Phys. Rev. D **89**, 104046 (2014).
[134] N. Bodendorfer and Y. Neiman, Imaginary action, spinfoam asymptotics and the "transplanckian" regime of loop quantum gravity, Classical Quantum Gravity **30**, 195018 (2013).
[135] A. Ghosh and D. Pranzetti, CFT/gravity correspondence on the isolated horizon, Nucl. Phys. **B889**, 1 (2014).
[136] D. Pranzetti and H. Sahlmann, Horizon entropy with loop quantum gravity methods, Phys. Lett. B **746**, 209 (2015).

[137] J. B. Achour, A. Mouchet, and K. Noui, Analytic continuation of black hole entropy in loop quantum gravity, J. High Energy Phys. 06 (2015) 145.

[138] J. B. Achour, K. Noui, and A. Perez, Analytic continuation of the rotating black hole state counting, J. High Energy Phys. 08 (2016) 149.

[139] L. Smolin, The strong and weak holographic principles, Nucl. Phys. **B601**, 209 (2001).

[140] L. Freidel, A. Perez, and D. Pranzetti, Loop gravity string, Phys. Rev. D **95**, 106002 (2017).

[141] K. Eder and H. Sahlmann, Quantum theory of charged isolated horizons, Phys. Rev. D **97**, 086016 (2018).

[142] N. Bodendorfer, Some notes on the Kodama state, maximal symmetry, and the isolated horizon boundary condition, Phys. Rev. D **93**, 124042 (2016).

[143] E. R. Livine and D. R. Terno, Reconstructing quantum geometry from quantum information: Area renormalisation, coarse-graining and entanglement on spin networks, arXiv:gr-qc/0603008.

[144] B. Dittrich, The continuum limit of loop quantum gravity: A framework for solving the theory, in *Loop Quantum Gravity: The First 30 Years*, edited by A. Ashtekar and J. Pullin (World Scientific, 2017), pp. 153–179.

[145] E. Alesci, M. Assanioussi, and J. Lewandowski, Curvature operator for loop quantum gravity, Phys. Rev. D **89**, 124017 (2014).

[146] T. Regge, General relativity without coordinates, Nuovo Cimento **19**, 558 (1961).

[147] J. Vines and D. A. Nichols, Properties of an affine transport equation and its holonomy, Gen. Relativ. Gravit. **48**, 127 (2016).